PALEOCEANOGRAPHY, VOL. 7, NO. 3, PAGES 357-389, JUNE 1992

EARLY AND MIDDLE MIOCENE STABLE ISOTOPES: IMPLICATIONS FOR DEEPWATER CIRCULATION AND CLIMATE

James D. Wright[1]

Lamont-Doherty Geological Observatory of Columbia University, Palisades, New York

Kenneth G. Miller[2]

Department of Geological Sciences, Rutgers University, New Brunswick, New Jersey

Richard G. Fairbanks[1]

Lamont-Doherty Geological Observatory of Columbia University, Palisades, New York

Abstract. The middle Miocene $\delta^{18}O$ increase represents a fundamental change in the ocean-atmosphere system which, like late Pleistocene climates, may be related to deepwater circulation patterns. There has been some debate concerning the early to early middle Miocene deepwater circulation patterns. Specifically, recent discussions have focused on the relative roles of Northern Component Water (NCW) production and warm, saline deep water originating in the eastern Tethys. Our time series and time slice reconstructions indicate that NCW and Tethyan outflow water, two relatively warm deepwater masses, were produced from ~20 to 16 Ma. NCW was produced again from 12.5 to 10.5 Ma. Another feature of the early and middle Miocene oceans was the presence of a high $\delta^{13}C$ intermediate water mass in the southern hemisphere, which apparently originated in the Southern Ocean. Miocene climates appear to be related directly to deepwater circulation changes. Deep-waters warmed in the early Miocene by ~3°C (~20 to 16 Ma) and cooled by a similar amount during the middle Miocene $\delta^{18}O$ increase (14.8 to 12.6 Ma), corresponding to the increase (~20 Ma) and subsequent decrease (~16 Ma) in the production of NCW and Tethyan outflow water. Large (>0.6 ‰), relatively rapid (~0.5 m.y.) $\delta^{18}O$ increases in both benthic and planktonic foraminifera (i.e., the Mi zones of Miller et al. (1991a) and Wright and Miller (1992a)) were superimposed on the long-term deepwater temperature changes; they are interpreted as reflecting continental ice growth events. Seven of these m.y. glacial/interglacial cycles have been recognized in the early to middle Miocene. Two of these glacial/interglacial cycles (Mi3 and Mi4) combined with a 2° to 3°C decrease in deepwater temperatures to produce the middle Miocene $\delta^{18}O$ shift.

INTRODUCTION

The Earth's climate has changed from the warm, equable conditions of the Cretaceous and early Eocene to the high-frequency northern hemisphere glacial-interglacial cycles that have dominated climates over the past 2.5 million years. The middle Miocene $\delta^{18}O$ increase was a major step in the progression toward cold polar climates. The prevailing interpretation from 1975 and through the early 1980s was that the middle Miocene $\delta^{18}O$ increase primarily recorded the initiation of continental glaciation on Antarctica [Shackleton and Kennett, 1975; Savin et al., 1975, 1981; Woodruff et al., 1981], i.e., the evolution of the "ice house" world. Matthews and Poore [1980] challenged this assumption and suggested that large ice sheets may have existed prior to the middle Miocene. Recent drilling in the Southern Ocean (ODP Legs 113, 114, 119, and 120 [Barker, et al., 1988; Ciesielski, P.F., et al. 1988; Barron, et al., 1989; Schlich, W.S., et al. 1989]) and on the Antarctic continental margins [Barrett et al., 1987] confirmed the existence of intermittent continental ice sheets on Antarctica between the early Oligocene and early Miocene [Miller et al., 1991a]. Still, the relative contributions from Antarctic ice growth and deepwater cooling to the middle Miocene $\delta^{18}O$ increase is uncertain. Furthermore, there is

[1]Also at Department of Geological Sciences, Columbia University, New York.

[2]Also at Lamont-Doherty Geological Observatory, Palisades, NY.

Paper number 92PA00760.
0883-8305/92/92PA-00760$10.00

disagreement as to whether this event represented the development of a permanent ice sheet in eastern Antarctica [cf. Matthews and Poore, 1980; Kennett and Barker, 1990].

Several hypotheses have linked climate changes to large-scale deepwater circulation changes. During the late Pliocene and Pleistocene, high fluxes of North Atlantic Deep Water (NADW) coincided with interglacial intervals, while low NADW fluxes occurred during glacial intervals [e.g., Shackleton et al., 1983; Boyle and Keigwin, 1982, 1987; Curry and Lohmann, 1982; Oppo and Fairbanks, 1987; Boyle, 1988; Curry et al., 1988; Duplessy et al., 1988; Oppo et al., 1990; Raymo et al., 1989]. Previous climate changes may have been related to deepwater circulation changes as well. Attempts to explain the middle Miocene $\delta^{18}O$ increase have called on changes in NCW [Schnitker, 1980] or Tethyan water [Woodruff and Savin, 1989]. However, there is little consensus concerning the early and middle Miocene deepwater circulation patterns (see below), hindering comparisons between climate and deepwater circulation during this interval. We clarify early to middle Miocene deepwater history by: (1) providing an early Miocene Southern Ocean benthic foraminiferal $\delta^{13}C$ record, which is critical for reconstructing deepwater circulation patterns [Oppo and Fairbanks, 1987; Wright et al., 1991; Charles and Fairbanks, 1992]; (2) improving stratigraphic correlations, which are necessary to ensure synoptic comparisons; and (3) integrating time series and time slice reconstructions to evaluate the timing, nature, and geographic extent of deepwater circulation changes.

MIOCENE DEEPWATER HYPOTHESES

Most workers agree that NCW was produced during parts of the late middle Miocene and that NCW flux was high in the late Miocene [Blanc et al., 1980; Schnitker, 1980; Miller and Fairbanks, 1985; Woodruff and Savin, 1989; Wright et al., 1991]. However, there is less concensus regarding the early and early middle Miocene deepwater circulation patterns [cf. Miller and Fairbanks, 1985; Woodruff and Savin, 1989]. Several workers have interpreted stable isotope and faunal changes to indicate that Northern Component Water (NCW, analogous to NADW) production initiated during the middle Miocene [e.g., Schnitker, 1980; Blanc et al., 1980; Woodruff and Savin, 1989]. An alternative to this idea was presented by Miller and Fairbanks [1985], who suggested that NCW was produced as early as the Oligocene. Extensive drift deposits in the northern North Atlantic support Miller and Fairbanks' conclusion at least for the early Miocene [Jones et al., 1970; Ruddiman, 1972; Roberts, 1975; Miller and Tucholke, 1983; Mountain and Tucholke, 1985]. Adding to the Miocene deepwater debate is the hypothesis that a warm, saline deepwater mass originated in the eastern Tethys during the early Miocene [Woodruff and Savin, 1989]. Four contrasting views on Miocene deepwater circulation and climate change are summarized below.

Blanc et al. [1980] and Schnitker [1980] proposed independently that the initial flux of NCW occurred when: (1) the Greenland-Scotland Ridge subsided to a critical depth below sea level; and (2) the eastern Tethys closed, shunting warm, salty water into the North Atlantic (a supposedly necessary component for NADW today [Reid, 1979]). Both cited evidence that these tectonic events occurred in the middle Miocene around 15 to 13 Ma. In relating the initiation of NCW to climate change, Schnitker [1980] proposed that southward transport of heat and salt via NCW enhanced evaporation in the Southern Ocean. He suggested that this led to increased moisture flux to Antarctica and initiated the development of a permanent ice sheet. The middle Miocene $\delta^{18}O$ increase was interpreted as evidence for continental ice growth and continued transport of heat to the Southern Ocean.

Woodruff and Savin [1989] proposed a different scenario for the middle Miocene $\delta^{18}O$ increase. They concurred with Schnitker [1980] that the middle Miocene $\delta^{18}O$ increase represented a buildup of ice on Antarctica and that NCW flux developed in the middle Miocene. However, their mechanism produced this ice growth through heat removal from the Antarctic coastal region. They suggested that prior to the middle Miocene $\delta^{18}O$ increase, heat was transported into the Southern Ocean through a turbulent plume of relatively warm, salty Tethyan water. They suggested that this excess heat flux to the high southern latitudes ameliorated the Antarctic continental climate and inhibited the development of a large continental ice sheet. Once the Tethyan seaway closed near 15 Ma, Antarctic climates cooled and ice growth began. Woodruff and Savin [1989] drew several conclusions about early and early middle Miocene deepwater circulation patterns: (1) Southern Component Water (SCW, analogous to Antarctic Bottom Water (AABW) [Broecker and Peng, 1982]) was the dominant water mass ventilating the deep oceans; (2) a warm, saline plume originated in the Tethys and was an important component of deepwater circulation and influence on climate; and (3) there is little evidence for NCW prior to 12 Ma.

Matthews and Poore [1980] and Prentice and Matthews [1988] argued that average tropical sea surface temperatures (SST's) were the most stable component of the climate system. Matthews and Poore [1980] proposed that planktonic foraminiferal $\delta^{18}O$ changes in western equatorial regions primarily reflected global seawater (δ_w) changes and that ice volume has been the dominant component of these changes since the middle Eocene. Their interpretation of the planktonic foraminiferal $\delta^{18}O$ record and that of Prentice and Matthews [1988] require that significant continental ice sheets (greater than or equal to modern ice volume) have been present since the late Eocene (~40 Ma). If these assumptions are correct, then deepwater temperatures were warmer than 10°C prior to the middle Miocene $\delta^{18}O$ increase. Both studies attributed the large middle Miocene $\delta^{18}O$ increase to a deepwater temperature decrease. Prentice and Matthews [1988] postulated that warm, saline water may have been an important component of deepwater circulation prior to that time.

In contrast to these studies, Miller and Fairbanks [1985] reported that North Atlantic $\delta^{13}C$ values were higher than those in the Pacific during much of the Miocene, arguing for the presence of NCW during this interval. Atlantic-Pacific $\delta^{13}C$ differences were ~0.5 ‰ during much of the early and middle Miocene versus the 1.0 ‰ difference observed today. Two intervals of large basin-basin $\delta^{13}C$ differences, 18 to 16 Ma and 12 to 10 Ma, corresponded to erosional events in the North Atlantic (Reflector R2 of Miller and Tucholke [1983] and Reflector Merlin of Mountain and Tucholke [1986], respectively). Miller and Fairbanks [1985] argued that the corroboration of the $\delta^{13}C$ data and the seismic stratigraphy indicated that these were intervals of peak NCW flux.

THE PROBLEM

Deepwater circulation patterns must be resolved to understand the cause of the middle Miocene $\delta^{18}O$ increase. The different scenarios presented above may result in a large part from different strategies and materials used in each study. For example, Miller and Fairbanks [1985] used $\delta^{13}C$ time series from the North Atlantic and Pacific. In contrast, Woodruff and Savin [1989] used all available isotope records, but they concentrated their data collection in the South Atlantic, Pacific, and Indian oceans. Their time slice approach portrayed cross-sectional changes in the ocean by averaging data for intervals of 1 to 2 m.y. duration.

Each study has limitations in its ability to resolve deepwater circulation patterns. Miller and Fairbanks' [1985] did not monitor vertical gradients or consider the Indian Ocean as a region for deepwater production. Woodruff and Savin's [1989] conclusions were largely influenced by high $\delta^{13}C$ values at intermediate depths in the Indian Ocean during the early Miocene. Much of these Indian Ocean data were adjusted because they were generated from the benthic foraminiferal genus *Oridorsalis*. This genus does not record the $\delta^{13}C$ value of the ambient water today. Also, by averaging the $\delta^{13}C$ data in 1 to 2 m.y. intervals, Woodruff and Savin's [1989] approach may produce artificial offsets or obscure real basin-basin differences. This can easily occur in the Miocene because of the large global changes in $\delta^{13}C$ values combined with different sample resolution at each site. In addition, both studies were hindered by biostratigraphic resolution, which can range from 0.5 to 2 m.y. for the Miocene [Miller and Kent, 1987]. We address these problems by improving stratigraphic control, which allows us to make refined time series and time slice reconstructions.

THE APPROACH AND STRATEGY

Modern Deepwater Formation and Circulation Patterns

The deepwater masses which ventilate the modern ocean are a product of surface water preconditioning (evaporation, cooling, and/or freezing) in the high latitudes. North Atlantic Deep Water (NADW) is produced in the Norwegian-Greenland and Labrador Seas, while Antarctic Bottom Water (AABW) originates in the Weddell Sea [Worthington, 1970; Foster and Carmack, 1976]. Although both water masses form in high latitudes, each deepwater mass has distinct characteristics which allow easy identification using temperature, salinity, and nutrient concentrations. NADW is composed largely of upper ocean water (surface and upper thermocline)

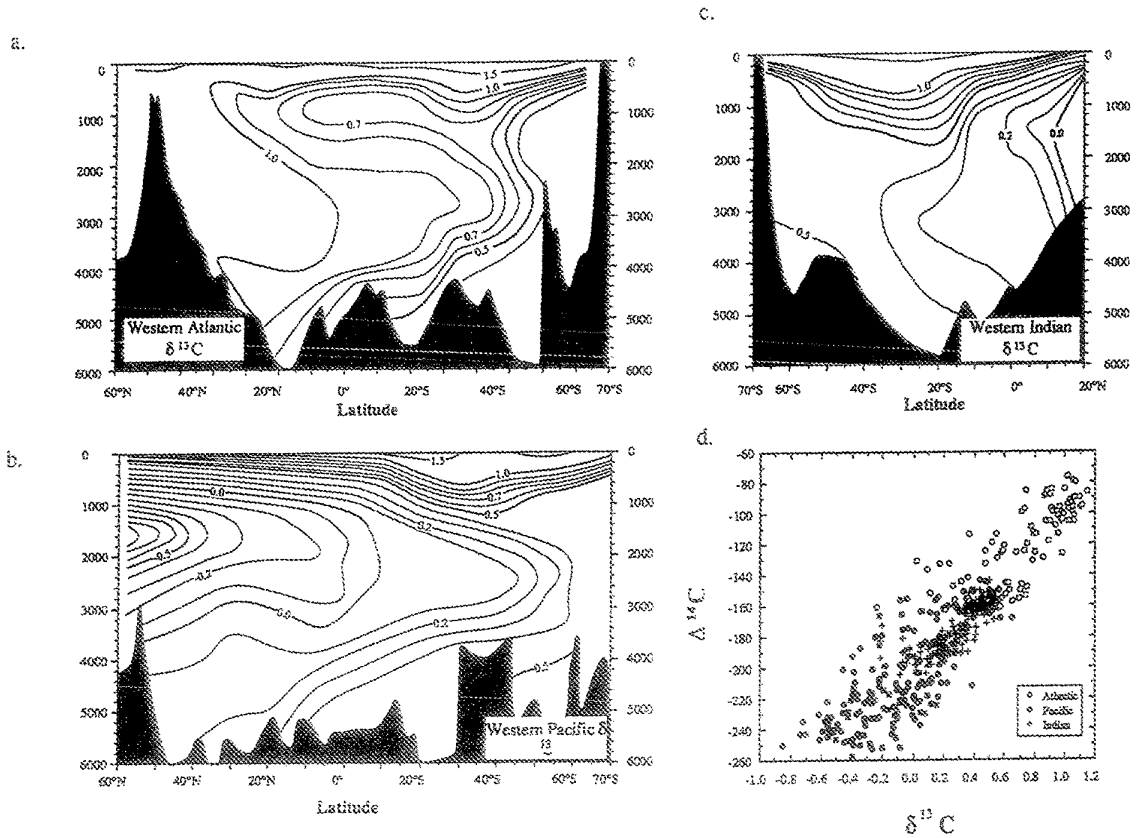

Fig. 1. GEOSECS $\delta^{13}C$ cross sections of the (a) western Atlantic, (b) western Pacific, and (c) western Indian (recontoured from Kroopnick [1985]). (d) $\Delta^{14}C$ versus $\delta^{13}C$ for the world's oceans greater than 2 km [after Broecker et al., 1990]. The Atlantic, Pacific, and Indian oceans $\Delta^{14}C$ and $\delta^{13}C$ data are from Ostlund et al. [1987].

[Worthington, 1970; Gordon and Piola, 1983] having a high $\delta^{13}C$ value (~1.0‰) (Figure 1) [Kroopnick, 1985]. However, only a small portion of Antarctic Bottom Water (AABW) is composed of surface water [Mantyla and Reid, 1983]; as a result, it has a lower $\delta^{13}C$ value (~0.4 ‰) (Figure 1).

Broecker et al. [1990] showed that there is a linear correlation between decreasing $\delta^{13}C$ and $\Delta^{14}C$ values after NADW sinks in the North Atlantic (Figure 1d). Two processes can change the distribution of $\delta^{13}C$ and $\Delta^{14}C$ values in the deep ocean: mixing between water masses with different $\delta^{13}C$ and $\Delta^{14}C$ compositions or deepwater aging. Carbon-isotope changes within the Atlantic Ocean represent mixing between high $\delta^{13}C$ and $\Delta^{14}C$ water (NADW) and lower $\delta^{13}C$ and $\Delta^{14}C$ water (Circumpolar Water (CPW)) (Figure 1). The effect of deepwater aging on $\delta^{13}C$ values within the Atlantic is negligible because the residence time of deep water in this ocean is short (~350 years) and productivity in the overlying surface ocean is low [Broecker and Peng, 1982].

In contrast to the Atlantic, the residence time of deep water within the Pacific Ocean is long, allowing remineralized organic matter to lower the $\delta^{13}C$ values of deep water. AABW flows north in the deepest Pacific, reaching the equatorial Pacific with little alteration to its initial $\delta^{13}C$ value (Figure 1). Deep water upwells in the North Pacific where the lowest $\delta^{13}C$ and $\Delta^{14}C$ values in the deep oceans are found (Figure 1). The intermediate depth North Pacific water represents the "end of the line" for deepwater circulation in the modern ocean. The return water to the Southern Ocean creates a mixing zone between the North Pacific intermediate water and CPW at intermediate and upper deepwater depths. This water mass is termed Pacific Outflow Water (POW) (Figure 1), which has low deepwater $\delta^{13}C$ values (-0.5 ‰) [Kroopnick, 1985]. Deepwater circulation in the modern Indian Ocean resembles the Pacific pattern. Indian Ocean deepwater $\delta^{13}C$ values are not as depleted as those in the Pacific because its reservoir size is smaller.

The Southern Ocean Approach

Late Pleistocene deepwater circulation changes can be reconstructed by using the Southern Ocean as a gauge to monitor the relative production of NADW and POW. In the Southern Ocean, a vigorous circumpolar circulation homogenizes outflow water from the Atlantic, Indian, and Pacific oceans, reflecting the relative contributions from each ocean [Oppo and Fairbanks, 1987; Oppo et al., 1990; Wright et al., 1991; Charles and Fairbanks, 1992]. The Southern Ocean is partitioned into upper and lower Circumpolar Water (CPW). The upper water mass can be modified by biological and air-sea exchange processes at the surface, thereby limiting its effectiveness as a monitor of circulation changes [Charles and Fairbanks, 1990]. However, there is little surface water influence on lower CPW. The $\delta^{13}C$ value of lower CPW represents the proportion of the outflow waters from the major ocean basins. Therefore changes in deepwater circulation patterns will be recorded in the deep Southern Ocean $\delta^{13}C$ record.

We can use the Southern Ocean as a deepwater monitor for the Miocene because circumpolar circulation around Antarctica began prior to the Miocene with the removal of two barriers: (1) subsidence of the Tasman Plateau in the early Oligocene [Weissel et al., 1977] and (2) opening of the Drake Passage during the late Oligocene [Barker and Burrell, 1977; Lawver et al., 1991; Wright and Miller, 1992b].

Methods of Deepwater Reconstruction

Benthic foraminiferal $\delta^{13}C$ time series and time slice reconstructions have been used successfully to infer late Pleistocene and deepwater circulation patterns [Shackleton et al., 1983; Boyle and Keigwin, 1982; 1987; Curry and Lohmann, 1982; Curry et al., 1988; Oppo and Fairbanks, 1987; Oppo et al., 1990; Duplessy et al., 1988]. There are advantages and disadvantages associated with both time series and time slice reconstructions. The timing of deepwater circulation changes can be best constrained by using a time series approach. In addition, a time series reconstruction allows an evaluation of the nature of the response, i.e., in an on-off mode, through a gradual change, or some other means. The limitation of a time series approach is that, in general, only a few records can be effectively compared at once. For example, it is difficult to monitor both basin-basin differences and vertical gradients using time series records. A time slice approach examines both vertical and interbasinal distributions at once. However, a time slice represents only a "snapshot" of the ocean circulation and provides a poor constraint on the timing and nature of climate transitions. In addition, time slices are sensitive to minor correlation problems, particularly during intervals of large global change. Times series are less sensitive to such uncertainties because the comparison of individual records facilitates evaluation of age uncertainties [e.g., Miller et al., 1986, Figure 5].

We use both approaches to reconstruct Miocene deepwater history. Time series comparisons were used to determine the timing of large-scale circulation changes. In this method, the outflow from the Atlantic, Pacific, and Indian oceans are each considered to be deepwater end-members. The Southern Ocean serves as our monitor of the relative changes among the three end-members [Oppo and Fairbanks, 1987]. Once the timing of deepwater circulation changes was established, time slice cross sections were constructed for times which represented different states of deepwater circulation.

Site Selection

The North Atlantic has been a potential source of cold deep water since the separation of Greenland and Scandinavia around 56 Ma and the connection of the Greenland Sea to the Arctic Ocean around 37 Ma [Vogt, 1972; Vogt and Avery, 1974; Talwani and Eldholm, 1977]. Deep Sea Drilling Project (DSDP) Site 563 was chosen to monitor the North Atlantic response during the early and middle Miocene. This site was drilled on the western flank of the mid-Atlantic Ridge and is located in the core of NADW today (Table 1; Figure 2). Paleodepths for the early to middle Miocene were 3200 to 3600 m (using the backtracking equations of Miller et al. [1989]). Advantages of this site include a relatively complete lower to middle Miocene section and excellent stratigraphic control [Miller et al., 1985]. Approximately one sample per meter was obtained from the lower and middle Miocene sections at Site 563 (this study) [Miller and Fairbanks, 1985], yielding a sample resolution of 50 to 100 kyr.

DSDP Site 289 was drilled on the Ontong Java Plateau (Table 1; Figure 2). It is located in the core of POW today. Paleodepths for this site during the early and middle Miocene

TABLE 1. Site Information

Site	Latitude	Longitude	Depth
71	04°28'N	140°19'W	4419
77	00°28'N	133°13'W	4291
206	32°00'S	165°27'E	3200
237	07°05'S	58°08'E	1623
238	11°09'S	70°32'E	2832
253	24°53'S	87°22'E	1962
279	51°20'S	162°32'E	3341
289	00°29'S	158°30'E	2206
317	11°00'S	162°15'W	2700
319	12°01'S	101°31'W	4296
357	30°00'S	35°33'W	2086
360	35°51'S	18°05'E	2949
366	05°41'N	19°51'W	2853
406	55°20'N	22°04'W	2958
408	63°22'N	28°54'W	1624
448	16°20'N	134°52'E	3483
470	28°55'N	117°31'W	3549
495	12°30'N	92°02'W	3600
516	30°16'S	35°17'W	1320
518	29°58'S	38°88'W	3944
522	26°07'S	05°08'W	4441
525	29°04'S	02°59'E	2470
526	03°07'S	03°08'E	1064
529	28°55'S	02°46'E	3035
553	56°06'N	23°32'W	2329
555	56°40'N	20°47'W	1659
558	37°46'N	37°21'W	3754
563	33°39'N	43°46'W	3796
574	04°12'S	133°19'W	4561
588	26°06'S	161°13'E	1533
590	31°10'S	163°21'E	1299
591	31°35'S	164°26'E	2131
608	42°50'N	23°05'W	3526
610	53°13'N	18°53'W	2417
667	04°34'N	21°55'W	3529
703	47°03'S	07°54'E	1796
704	46°53'S	07°25'E	2531
709	03°54'S	60°33'E	3049
714	05°04'N	73°47'E	2083
744	61°35'S	80°36'E	2318
747	54°49'S	76°48'E	1706

were calculated to be ~2300 m. Stable isotope data for Site 289 have been generated by Savin et al. [1981, 1985] and Woodruff and Savin [1989, 1991]. Site 289 has a thick, complete Miocene section, although the existing stable isotope data do not include the earliest Miocene (circa 23.6 to 21 Ma).

The early Miocene Southern Ocean is represented by Ocean Drilling Program (ODP) Site 704, which was drilled on the Meteor Rise (Table 1, Figure 2) [Ciesielski et al., 1988]. Site 704 contains approximately 135 m of lower Miocene sediments. Early Miocene paleodepths are estimated to be 2350 to 2450 m. The middle Miocene section is not represented at Site 704. Approximately 1 sample per 2 m from Site 704 was analyzed, yielding an average sample resolution of 50 kyr. Kerguelen Plateau Sites 747 [Wright and Miller, 1992a] and 751 [Mackensen et al., 1992] have complete middle Miocene sections, but their paleodepths (1400-1600 m) cannot ensure isolation from surface or intermediate water influences. Woodruff and Chambers [1991] and Barrera and Huber [1991] analyzed the benthic foraminiferal stable isotopes from Site 744 on the southern end of the Kerguelen Plateau. This site is well suited for this study, but the present sample resolution is not adequate for our needs.

DSDP Site 237 was recovered from the Mascarene Plateau (Table 1, Figure 2). Early and middle Miocene paleodepths for this site are estimated to have been 1250-1350 m [Sclater et al., 1985]. The lower Miocene section is only 28.5 m thick at this site and sedimentation rates were low (3-4 m/m.y.). Despite this, upper lower and lower middle Miocene isotopic resolution at this site is sufficient to evaluate the Indian Ocean's role in deepwater circulation using Woodruff and Savin's [1991] stable isotope record from *Cibicidoides* spp. at this site.

Time slice reconstructions only require a short interval containing the appropriate time horizon, in contrast to a time series approach which requires relatively continuous and geographically well-positioned stable isotope records. More sites can be included in the time slice reconstructions. Therefore stable isotope records were considered from a large number of sources (Table 2). The primary goal of the time slice reconstruction was to contrast the three major ocean basins during different modes of operation. However, large changes in the mean ocean $\delta^{13}C$ value require precise stratigraphic control to ensure synoptic comparisons. Therefore the time slices selected were also based on our confidence in recognizing a particular time horizon (see stratigraphy). Locations of all sites used in time series and time slice reconstructions are shown in Figure 2.

Measurements

Benthic foraminiferal isotopic analyses were performed on *Cibicidoides* spp. (including *Planulina wuellerstorfi*), which secrete tests constantly offset from $\delta^{18}O$ equilibrium and reflect the $\delta^{13}C$ gradients of the ambient water [Shackleton and Opdyke, 1973; Duplessy et al., 1970; Woodruff et al., 1980; Belanger et al., 1981; Graham et al., 1981]. Stable isotope data were generated for Sites 360 (Cape Basin, 2949 m present depth, 3000-2950 m paleodepths; Figure 3), 553 (Rockall Plateau, 2339 present depth, 1930-2250 m paleodepths; Figure 4), 563 (Figure 5), 608 (eastern North Atlantic, 3526 m present depth, 3100-3400 m paleodepths; Figure 6), and 704 (Figure 7). Samples were analyzed by a Carousel-48 automatic carbonate preparation device attached to a Finnigan MAT 251 mass spectrometer. The data were corrected to the NBS-19 (-2.19 and 1.92 ‰ for $\delta^{18}O$ and $\delta^{13}C$) and NBS-20 (-4.14 and -1.06 ‰ for $\delta^{18}O$ and $\delta^{13}C$) standards. Results are reported relative to the peedee belemnite (PDB) standard (Table 3, Figures 4-7). All cross-sectional reconstructions considered only *Cibicidoides* and *Planulina* data.

Stratigraphic Control

A uniform scheme for age assignments is necessary to correlate isotope records from different ocean basins. The most unequivocal method is to correlate to the Geomagnetic Polarity Time Scale (GPTS) [Berggren et al., 1985] (for examples, see Miller et al., 1985, 1988, 1991b). However, paleomagnetic records are unreliable for equatorial and older DSDP sites. Sites without polarity data were calibrated to the GPTS using isotope stratigraphy. Nine benthic foraminiferal $\delta^{18}O$

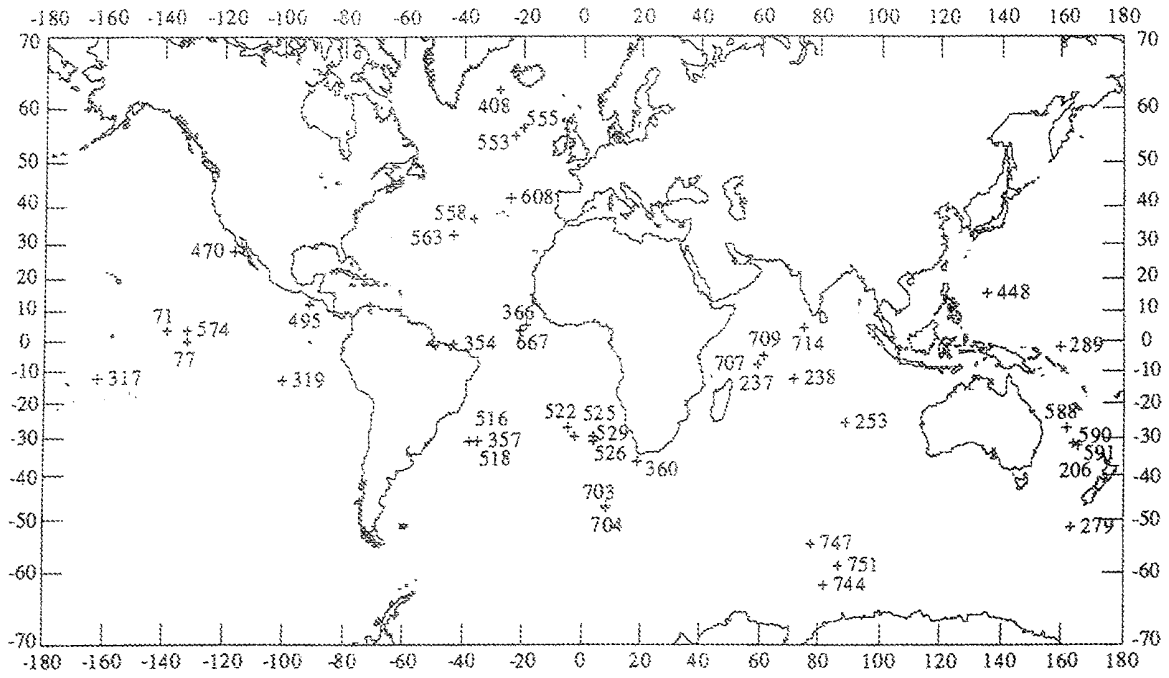

Fig. 2. Locations of DSDP and ODP sites used in time series and time slice reconstructions.

TABLE 2a. Data Used in the Oligocene/Miocene Boundary Time Slice Reconstruction (Zone Mi1 - 23.7 Ma)

Site	Depth (mbsf)	Paleo-latitude	Paleo-depth	$\delta^{18}O$	$\delta^{13}C$	Source
			Atlantic			
366	255.39	6°N	2533	1.71	1.42	Miller et al. [1989]
522	56.93	26°S	3759	2.23	1.64	Miller et al. [1988]
529	108.50	29°S	2625	1.98	1.36	Miller et al. [1987]; Woodruff and Savin [1991]
553	233.61	56°N	1932	1.37	0.63	this study
563	301.67	34°N	3213	2.05	1.59	this study
608	411.36	43°N	3115	1.61	1.38	this study
667	270.80	5°N	3218	1.74	1.40	Miller et al. [1989]; Woodruff and Savin [1991]
703	43.62	47°S	1317	1.90	1.44	Miller [1992]
704	578.67	47°S	2351	2.32	1.86	this study
			Pacific			
317	230.16	17°S	2463	2.22	1.40	Woodruff and Savin [1989]
588	388.80	35.5°S	1348	1.81	1.57	Kennett [1986]
			Indian			
744	98.46	61°S	2024	2.27	1.35	Barrera and Huber [1991]
747	127.90	55°S	1433	1.88	1.43	Wright and Miller [1992a]

TABLE 2b. Data Used in the Early Miocene Time Slice Reconstruction (Zone Mi1b - 18.3 Ma)

Site	Depth (mbsf)	Paleo-latitude	Paleo-depth	$\delta^{18}O$	$\delta^{13}C$	Source
			Atlantic			
366	198.06	6°N	2623	1.90	0.34	Miller et al. [1989]
555	272.26	57°N	1414	1.11	0.91	this study
563	268.24	34°N	3403	1.64	1.17	this study
608	349.16	43°N	3252	1.55	0.91	this study
667	208.60	5°N	3305	1.68	0.72	Miller et al. [1989]
704	474.20	47°S	2421	1.63	0.57	this study
			Pacific			
77	253.70	4°S	3834	1.61	0.61	Savin et al. [1981]; Woodruff and Savin [1989]
289	540.25	5°S	2319	1.85	0.55	Savin et al. [1981]; Woodruff and Savin [1989]
317	175.50	15.5°S	2500	1.72	0.78	Woodruff and Savin [1989]
588	337.80	33°S	1426	1.37	1.24	Kennett [1986]
			Indian			
237	181.53	9°S	1298	1.95	1.11	Woodruff and Savin [1991]
253	81.15	32°S	1502	2.00	0.96	Oberhänsli [1986]
709	172.25	6°S	2708	2.10	0.89	Woodruff et al. [1990]
744	77.09	61°S	2085	1.97	1.40	Barrera and Huber [1991]
747	96.40	55°S	1505	1.65	1.10	Wright and Miller [1992a]

TABLE 2c. Data Used in the Early Middle Miocene Time Slice Reconstruction (Zone Mi2 - 16.2 Ma)

Site	Depth (mbsf)	Paleo-latitude	Paleo-depth	$\delta^{18}O$	$\delta^{13}C$	Source
			Atlantic			
366	159.23	6°N	2645	1.54	1.76	Miller et al. [1989]
516	93.98	30°S	1131	0.86	2.15	Woodruff and Savin [1989]
518	65.60	30°S	3746	1.69	1.70	Woodruff and Savin [1989]
558	292.31	38°N	3415	1.56	2.08	Miller and Fairbanks [1985]
563	248.93	34°N	3465	1.64	2.07	this study
608	331.40	43°N	3304	1.46	1.99	this study
667	183.66	5°N	3334	1.59	1.79	Miller et al. [1989]
			Pacific			
71	187.50	0°	4112	1.70	1.61	Woodruff and Savin [1989]
77	243.02	3.5°S	3910	1.44	1.44	Savin et al. [1981]; Woodruff and Savin [1989]
289	472.40	4.5°S	2307	1.55	1.71	Savin et al. [1981]; Woodruff and Savin [1989]
317	165.23	15°S	2519	1.87	1.61	Woodruff and Savin [1989]
319	107.40	16°S	3475	1.88	1.73	Woodruff and Savin [1989]
448	16.40	16°N	2938	1.46	1.40	Woodruff and Savin [1989]
495	236.90	12°N	3478	1.92	1.63	Barrera et al. [1985]
574	192.47	8°S	4158	1.98	1.69	Woodruff and Savin [1989]
588	314.30	32.5°S	1453	1.30	1.95	Kennett [1986]
			Indian			
237	159.20	9°S	1337	1.76	1.95	Woodruff and Savin [1991]
709	141.65	6°S	2744	1.78	1.93	Woodruff et al. [1990]
744	64.74	61°S	2125	1.90	1.90	Woodruff and Chambers [1991]
747	84.90	55°S	1532	1.42	1.76	Wright and Miller [1992a]

TABLE 2d. Data Used in the Middle Miocene Time Slice Reconstruction (Zone Mi3 - 13.6 Ma)

Site	Depth (mbsf)	Paleo-latitude	Paleo-depth	$\delta^{18}O$	$\delta^{13}C$	Source
			Atlantic			
357	52.03	30°S	1925	2.03	1.79	Woodruff and Savin [1989]
360	303.55	35°S	2995	1.99	1.87	this study
408	260.00	63°N	1189	1.76	1.60	Keigwin et al. [1986]
525	190.50	29°S	2321	1.94	2.14	Woodruff and Savin [1991]
553	220.03	56°N	2175	1.90	1.58	this study
563	235.14	34°N	3542	1.96	1.72	Miller and Fairbanks [1985]
608	297.70	43°N	3358	1.74	1.74	this study
			Pacific			
77	228.43	3°S	3994	1.48	1.43	Savin et al. [1981]; Woodruff and Savin [1989]
206	284.10	35.5°S	3115	2.77	1.36	Woodruff and Savin [1989]
289	444.49	4°S	2322	2.22	1.67	Savin et al. [1981]; Woodruff and Savin [1989]
317	148.78	14.5°S	2543	2.28	1.28	Woodruff and Savin [1989]
470	163.52	27°N	2785	2.21	1.11	Barrera et al. [1985]
495	205.85	12°N	3634	1.65	0.91	Barrera et al. [1985]
574	152.41	7.5°S	4226	2.30	1.93	Woodruff and Savin [1989]
588	280.50	31.5°S	1479	1.61	1.98	Kennett [1986]
590	436.80	36.5°S	1334	1.41	2.11	Kennett [1986]
591	441.00	36.5°S	2170	1.87	1.91	Kennett [1986]
			Indian			
237	149.23	8.5°S	1397	2.02	1.57	Woodruff and Savin [1991]
253	68.65	30.5°S	1638	1.93	1.72	Oberhänsli [1986]
709	126.75	5.5°S	2800	2.22	1.79	Woodruff et al. [1990]
714	77.00	1°N	1763	1.95	1.12	Boersma and Mikkelsen [1990]
744	57.75	61°S	2161	1.91	1.88	Woodruff and Chambers [1991]
747	70.00	55°S	1563	1.83	1.79	Wright and Miller [1992a]

increases have been used to define the bases of nine Miocene isotope zones (Figure 8) [Miller et al., 1991a; Wright and Miller, 1992a]. By correlating these $\delta^{18}O$ increases at three sites from different ocean basins to the same magnetochrons, we established that these events were globally synchronous.

For sites without a polarity record, we first used the published biostratigraphy for each site and the magnetobiostratigraphic ages of Berggren et al. [1985] to establish general age estimates. Once a basic stratigraphic framework was established, $\delta^{18}O$ maxima were identified and assigned ages based on correlation with $\delta^{18}O$ maxima of the standard sections [Miller et al., 1991a; Wright and Miller, 1992a]. By using $\delta^{18}O$ correlations, more precise (much better than 0.5 m.y.) site to site correlations are established, ensuring synoptic time slice reconstructions. The Mi Zonations of Miller et al. [1991a] and Wright and Miller [1992a] are used as correlation points for age estimation. In Table 2, we have listed the depths of the "Mi" Zones at each site used in the time slice reconstructions.

Backtracking

The paleobathymetry of all locations was considered carefully, using backtracking techniques and equations discussed by Miller et al. [1986, 1989]. Almost all sites were drilled on oceanic crust and were backtracked using a simple thermal subsidence model. Only Kerguelen Plateau Sites 744 and 747 presented a problem in using these simple thermal subsidence models. The uplift history of this plateau is complicated and not well understood. However, there is evidence that Site 747 was near sea level at 75 Ma [Schlich et al., 1989]. If these sites were near sea level at 75 Ma, then a simple exponential decay function from Parsons and Sclater [1977] predicts a water depth for the present that is within 100 m of the actual present depth. The resulting Miocene paleodepth estimates range from 1400 to 1600 m for the early and middle Miocene.

The paleolatitudinal positions have changed since the early and middle Miocene. The Indian Ocean sites displayed the most latitudinal movement. Paleolatitudinal reconstructions for this ocean were based on a linear interpolation between the reconstructed paleopositions for anomaly 13 (~36 Ma) and the present [Sclater et al., 1977a]. The Pacific paleolatitudes were determined by using the Sclater et al.'s [1985] plate reconstructions for anomalies 6 (~20 Ma) and 5 (~9 Ma). Paleolatitudinal positions of Atlantic sites were considered to be similar to the present [Sclater et al., 1977b].

TABLE 2e. Data Used in the Late Middle Miocene Time Slice Reconstruction (Zone Mi5 - 11.3 Ma)

Site	Depth (mbsf)	Paleo-latitude	Paleo-depth	$\delta^{18}O$	$\delta^{13}C$	Source
			Atlantic			
357	39.52	30°S	1951	1.43	1.61	Woodruff and Savin [1989]
360	265.11	36°S	2996	2.13	0.84	this study
408	202.86	63°N	1290	1.90	1.16	Keigwin et al. [1986]
525	149.57	29°S	2350	2.28	1.75	Shackleton et al. [1984]
526	105.11	29°S	903	2.29	1.77	Shackleton et al. [1984]
553	208.80	56°N	2220	2.10	1.04	this study
555	168.24	56°N	1517	1.99	1.40	this study
563	199.34	34°N	3593	2.06	1.48	this study
608	252.01	43°N	3394	2.20	1.35	this study
			Pacific			
77	182.28	2°S	4048	2.26	1.00	Savin et al. [1981]; Woodruff and Savin [1989]
206	232.10	35°S	3132	2.04	1.36	Woodruff and Savin [1989]
289	367.66	3.5°S	2304	2.55	1.09	Savin et al. [1981]; Woodruff and Savin [1989]
470	~110.0	27.5°N	2968	2.67	0.63	Barrera et al. [1985]
574	98.13	7°S	4273	2.69	1.09	Woodruff and Savin [1989]
588	246.00	30.5°S	1499	1.73	1.36	Kennett [1986]
590	388.8	35.5°S	1348	2.17	1.45	Kennett [1986]
591	366.30	35.5°S	2167	2.08	1.41	Kennett [1986]
			Indian			
237	132.13	8°S	1447	2.43	0.84	Woodruff and Savin [1991]
238	261.66	13°S	2617	2.90	1.46	Vincent et al. [1980]
253	57.65	30°S	1699	2.43	1.30	Oberhänsli [1986]
709	117.65	5°S	2850	2.59	1.05	Woodruff et al. [1990]
714	67.30	1.5°N	1808	2.16	1.14	Boersma and Mikkelsen [1990]
744	45.61	61°S	2187	2.51	1.36	Woodruff and Chambers [1991]
747	59.04	55°S	1590	2.49	1.43	Wright and Miller [1992a]

Diagenesis

Diagenesis may overprint or erase the isotopic composition recorded originally by foraminifera. Several studies have documented that diagenesis may be a problem in deeply buried sections (>400 m) [Miller and Curry, 1982; Miller et al., 1987; Barrera et al., 1987]. Diagenetic alteration is not considered to have overprinted the isotope records in this study because most of the sections were not deeply buried. However, the lower Miocene section at Site 704 lies between 435 and 600 mbsf. Two criteria were used to discriminate against diagenetically altered samples: (1) optical evidence for overgrowths and (2) consistency among isotopic records. Initially, the lower Miocene section at Site 704 was suspected to have been altered based on the high burial depths. However, there was no optical evidence for overgrowths on the benthic foraminiferal tests and the $\delta^{18}O$ record from this interval was nearly identical to the less deeply buried records from Sites 563 and 747.

RESULTS - SNAP SHOTS AND MOTION PICTURES

Benthic foraminiferal $\delta^{13}C$ values record the mean ocean $\delta^{13}C$ value which responded to changes in the input/output ratio of inorganic carbon to organic carbon through time [Miller and Fairbanks, 1985; Vincent and Berger, 1985; Shackleton, 1987; Delaney and Boyle, 1987]. Superimposed on the mean ocean $\delta^{13}C$ value are basin to basin and vertical differences in $\delta^{13}C$ values which result from thermohaline circulation patterns. Large changes in the mean ocean $\delta^{13}C$ values (1.0-1.5 ‰) occurred during the Miocene and were often larger than the circulation induced end-member range (0.5 to 1.0 ‰). However, site-to-site $\delta^{13}C$ differences must reflect circulation patterns because changes in the mean ocean $\delta^{13}C$ value were recorded at all sites.

Deepwater circulation reconstructions using $\delta^{13}C$ monitor deepwater mixing and/or aging after leaving their source regions. "Young" deep waters, such as NCW and Tethyan water masses, may be detected by their high $\delta^{13}C$ values because they have a large surface waters component. We found no evidence for Pacific deepwater production during the Miocene, which is in agreement with Woodruff and Savin [1989] but contrary to the findings of Blanc and Duplessy [1982]. The history of SCW is more problematic because its $\delta^{13}C$ values are less distinct in comparison to NCW and POW values.

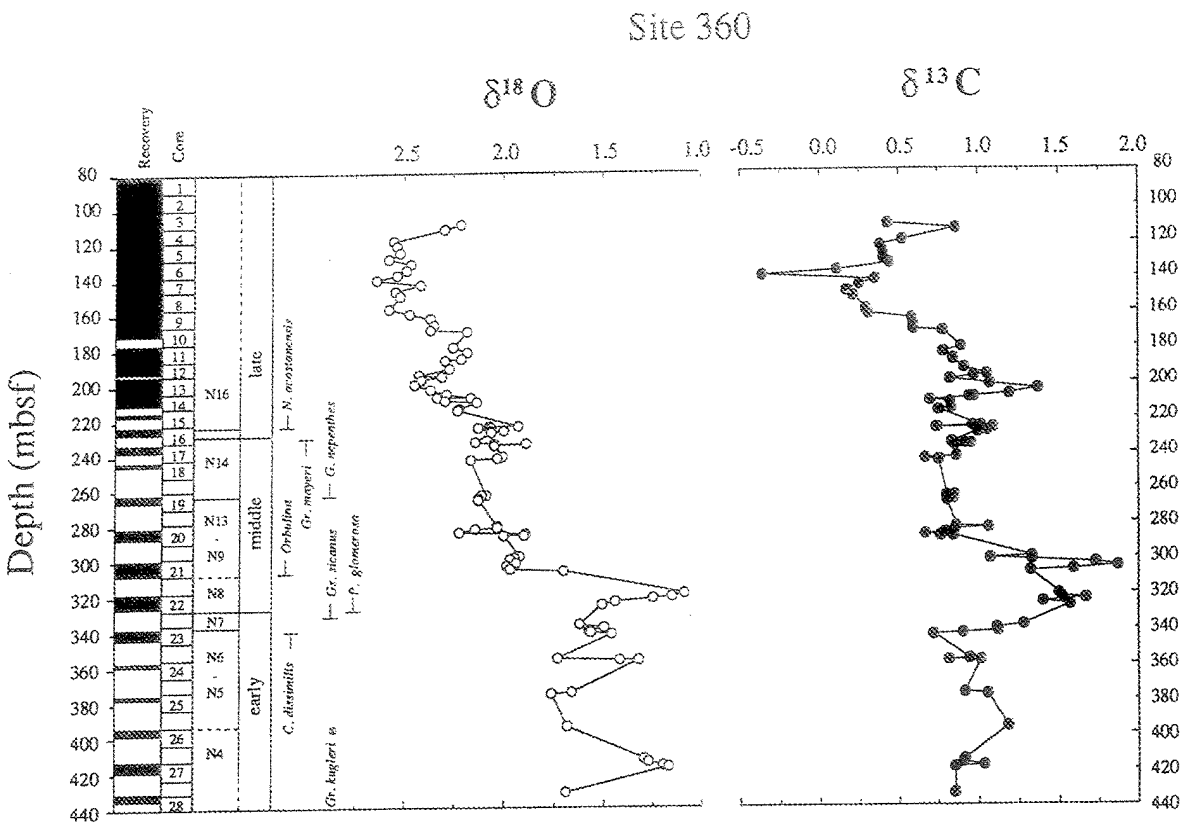

Fig. 3. Site 360 (Cape Basin) $\delta^{18}O$ and $\delta^{13}C$ isotope data plotted versus depth.

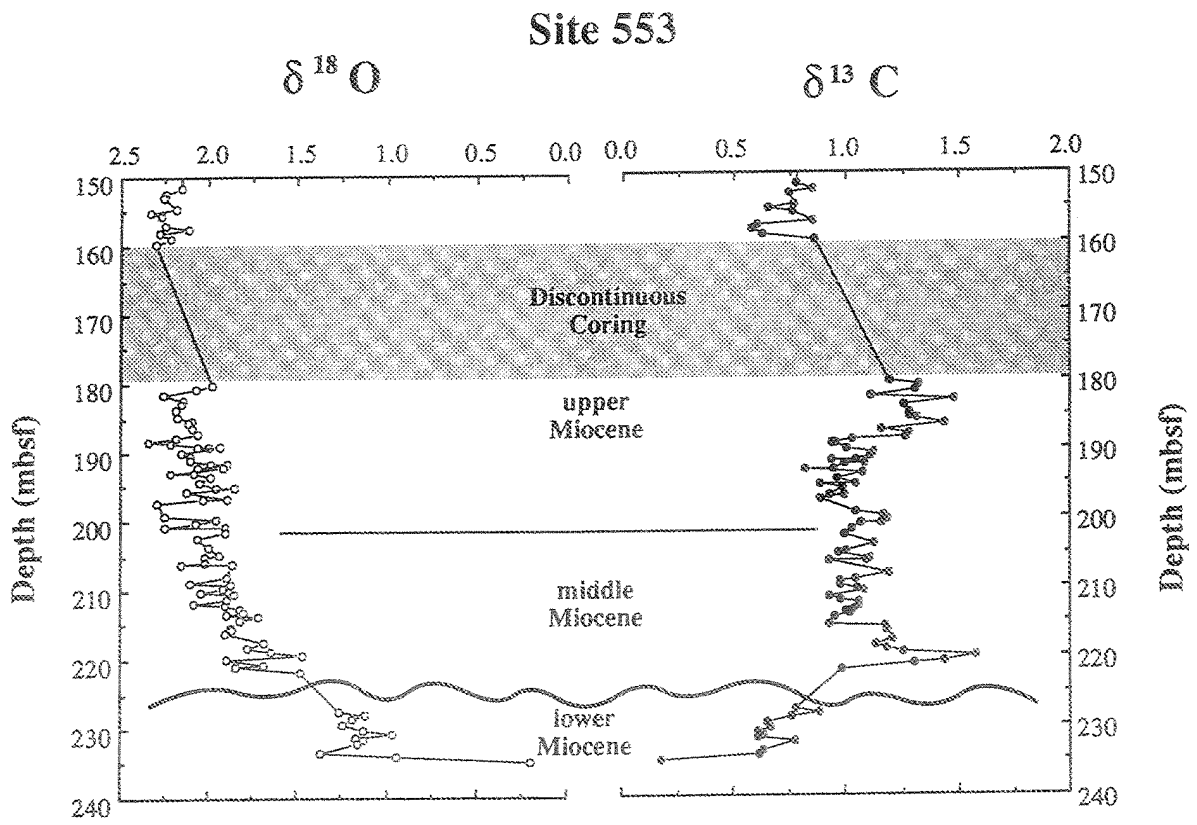

Fig. 4. Site 553 (Rockall Plateau) $\delta^{18}O$ and $\delta^{13}C$ isotope data plotted versus depth.

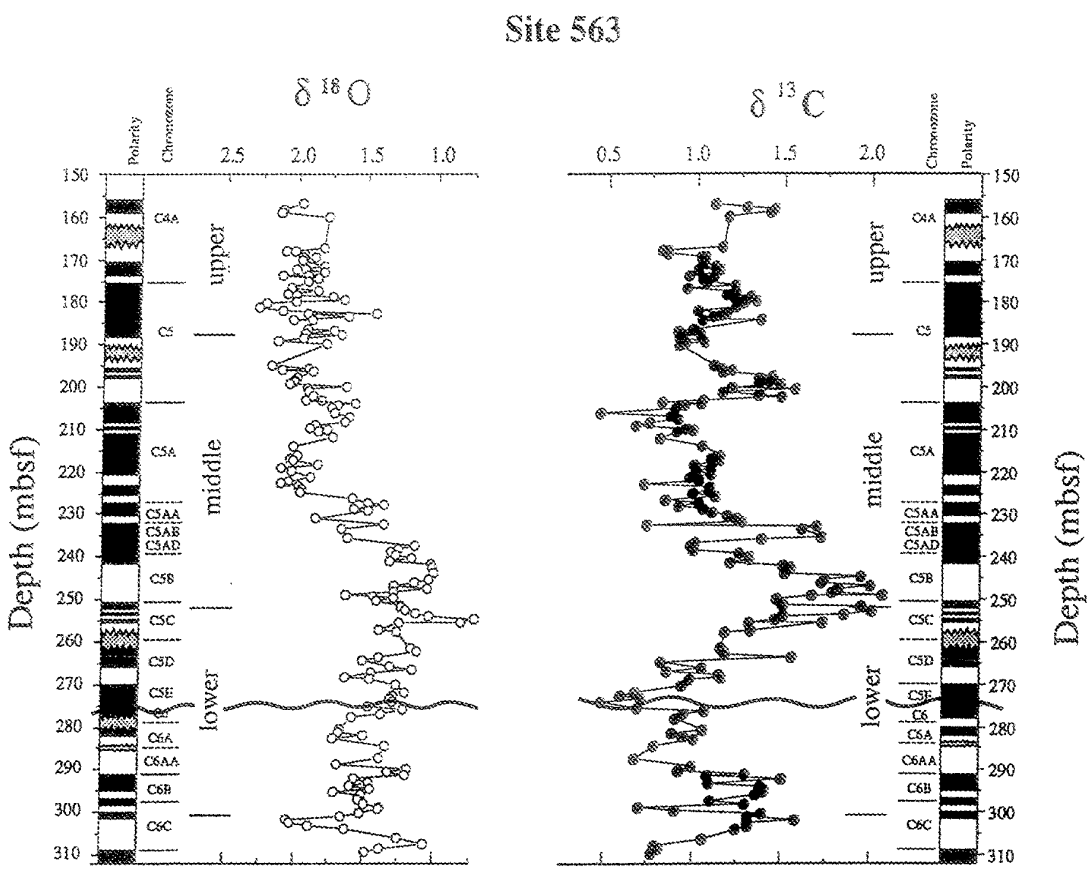

Fig. 5. Site 563 (North Atlantic) $\delta^{18}O$ and $\delta^{13}C$ isotope data plotted versus depth.

Early Miocene Time Series

Core coverage and hence deep-sea stable isotope and faunal coverage of the earliest Miocene (~24 to 21 Ma) is poor; as a result, deepwater circulation patterns are not well documented for this interval. However, there are sufficient data to evaluate the role of the North Atlantic during the earliest Miocene. In this interval, Southern Ocean $\delta^{13}C$ values (Site 704) were always as high as or higher than values in the deep North Atlantic (Site 563) (Figure 9). Equivalent $\delta^{13}C$ values in the North Atlantic and Southern Ocean imply that SCW filled the deep North Atlantic, while higher values in the Southern Ocean indicate deepwater aging within the Atlantic. Both relationships resulted from little or no NCW production. These conditions prevailed until at least 21 Ma (Figure 9).

The early Miocene global $\delta^{13}C$ increase (the Monterey Event as discussed by Vincent and Berger [1985]) spanned the interval from approximately 19 to 16 Ma. Carbon isotope values at North Atlantic Site 563 were consistently higher than those at Pacific Site 289 during this $\delta^{13}C$ increase (Figure 9). The $\delta^{13}C$ values increased from 0.5 to 2.1 ‰ in the North Atlantic (Site 563) and from 0.1 to 1.7 ‰ in the Pacific (Site 289); both sites recorded a 1.6 ‰ change over the 3 m.y. interval. Southern Ocean Site 704 recorded $\delta^{13}C$ values intermediate between the North Atlantic and Pacific during this interval (Figure 9). A high $\delta^{13}C$ water mass must have originated in the North Atlantic and/or Indian oceans between 19 and 16 Ma to produce Southern Ocean $\delta^{13}C$ values higher than those in the Pacific (Figure 9). North Atlantic $\delta^{13}C$ values were higher than those in the Southern Ocean, establishing that the northern North Atlantic was a deepwater source from 19 to 16 Ma.

The Indian Ocean also remains as a possible source of high $\delta^{13}C$ water for the late early Miocene [Woodruff and Savin, 1989]. Site 237 provides the best record to evaluate the Indian Ocean's role. This site recorded $\delta^{13}C$ values similar to those in the deep North Atlantic and higher than those in the Southern Ocean (Figure 10). This indicates that the northern Indian Ocean or eastern Tethyan region was an additional source of high $\delta^{13}C$ water to the Southern Ocean from 19 to 16 Ma, confirming the hypothesis of Woodruff and Savin [1989].

The $\delta^{13}C$ evidence indicates that NCW and Tethyan outflow water were produced between 19 and 16 Ma (Figures 9 and 10). Production may have begun earlier, but the timing is masked by a regional hiatus recorded at Site 563 from 21 to 19 Ma and poor sample resolution at Site 237. Erosion in the northern

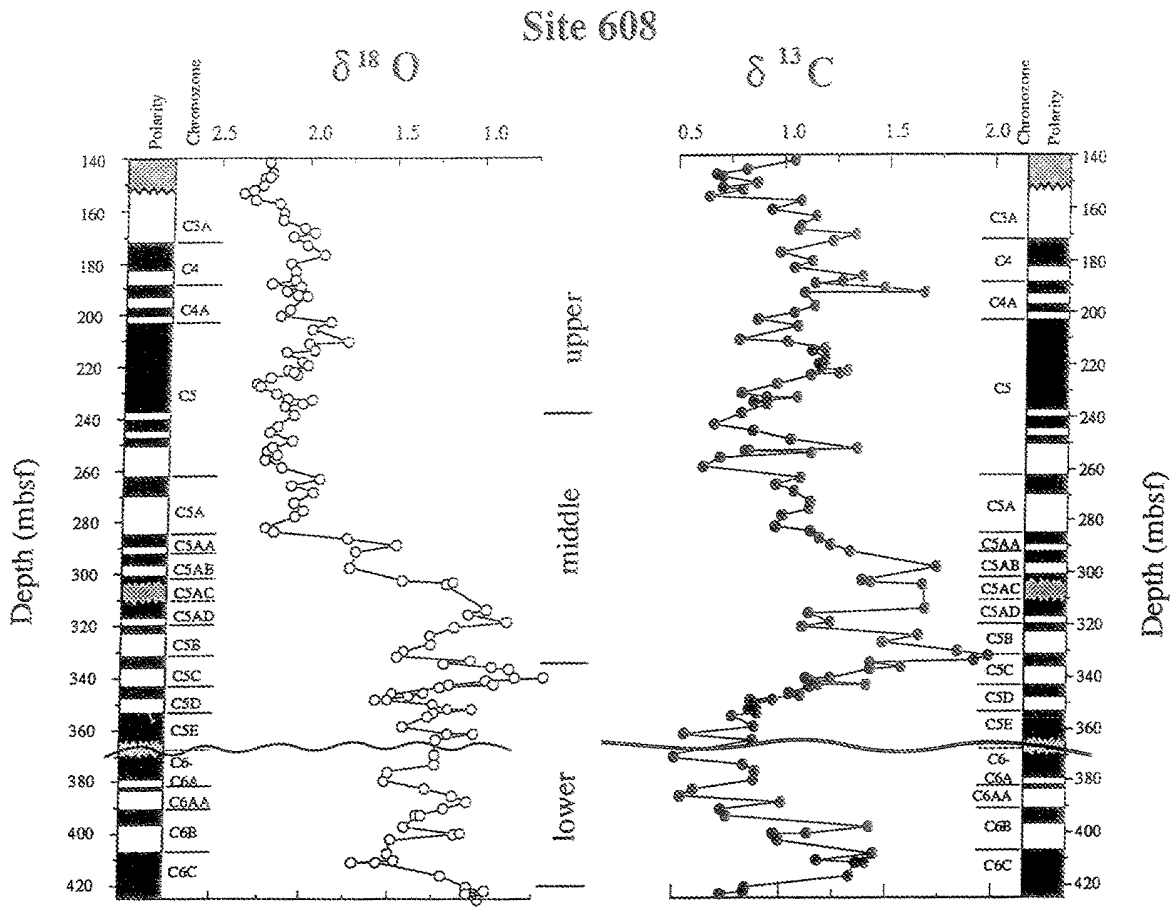

Fig. 6. Site 608 (Cape Basin) $\delta^{18}O$ and $\delta^{13}C$ isotope data plotted versus depth.

North Atlantic from 21 to 19 Ma provides additional evidence for a NCW pulse (Reflector R2 of Miller and Tucholke [1983]). Constraints can be placed on the timing of NCW and/or Tethyan production by using $\delta^{13}C$ values recorded in the Pacific (Site 289) and Southern oceans (Site 704). From approximately 21 to 20 Ma, the Southern and Pacific oceans recorded similar $\delta^{13}C$ values (Figure 9), implying that there was little to no high $\delta^{13}C$ contribution from the Atlantic or Indian oceans. Carbon isotope values in the Southern Ocean diverged from those in the Pacific at 19.5 Ma (Figure 9), indicating that NCW production and/or Tethyan outflow began at 19.5 Ma.

Early Miocene Time slices

During the early Miocene, deepwater circulation patterns changed from a one component system dominated by SCW to a three-component system with the addition of NCW and Tethyan fluxes. Three time slices were selected to verify this interpretation of the changing deepwater circulation patterns. The first cross section reconstruction examined the ocean at Oligocene/Miocene boundary (23.7 Ma). This time slice was selected because it represents a time during which time series indicate that only SCW filled the deep oceans. In addition, this time slice can be identified by a distinct $\delta^{18}O$ maximum which is used to define the base of Miocene Isotope Zone Mi1 [Miller et al., 1991a; Wright and Miller, 1992a]. A second time slice was selected to reconstruct the ocean near the beginning of the global carbon isotope increase (Monterey Event). This time slice is within the interval when both NCW and Tethyan fluxes have been inferred. Oxygen Isotope Zone Mi1b (18.3 Ma) serves as the marker for reconstruction of this cross section. A third time slice near the early/middle Miocene boundary was selected because it is within an interval interpreted to have a high flux of NCW. This time slice occurs at the base of Oxygen Isotope Zone Mi2 (16.2 Ma) and represents the carbon-isotope maximum of the Monterey Event [Vincent and Berger, 1985].

The Oligocene/Miocene boundary (Zone Mi1, 23.7 Ma). The Oligocene/Miocene boundary reconstruction epitomizes an ocean without a NCW source (Figure 11). The Atlantic Ocean was dominated by a SCW flux, producing a south to north $\delta^{13}C$ gradient. The lowest $\delta^{13}C$ values in this time slice were recorded at Rockall Plateau Site 553 (Figure 11). This suggests that either: (1) climatic conditions were not conducive to deep convection in the Norwegian-Greenland Sea or the

TABLE 3. Unpublished $\delta^{18}O$ and $\delta^{13}C$ Data From Sites 360, 553, 555, 563, 608, and 704B

Sample	Depth	Age	$\delta^{18}O$	$\delta^{13}C$
		Site 360		
19-2 130-134	262.80	11.37	2.09	0.80
19-3 21-25	263.21	11.39	2.12	0.85
19-4 60-64	265.11	11.49	2.13	0.84
19-4 111-115	265.61	11.52	2.13	0.80
20-1 146-150	280.46	12.30	2.04	0.86
20-2 85-89	281.35	12.34	2.04	1.06
20-3 89-93	282.89	12.42	2.15	0.85
20-4 93-97	284.43	12.50	2.23	0.79
20-5 20-24	285.20	12.54	1.89	0.66
20-5 83-87	285.83	12.58	1.90	0.76
20-5 145-149	286.45	12.61	2.00	0.84
21-1 15-19	298.15	13.22	1.92	1.33
21-1 92-96	298.92	13.26	1.95	1.07
21-2 73-77	300.23	13.33	1.97	1.33
21-3 106-110	302.06	13.43	1.94	1.73
21-4 105-109	303.55	13.51	1.99	1.87
21-5 91-95	304.91	13.58	1.97	1.59
21-6 73-77	306.23	13.65	1.70	1.32
22-2 100-104	319.50	17.00	1.09	1.50
22-3 134-138	321.34	17.07	1.15	1.52
22-3 142-146	321.42	17.08	1.25	1.67
22-5 83-87	323.83	17.17	1.44	1.40
22-6 58-62	325.08	17.22	1.51	1.57
23-1 86-90	336.86	17.69	1.62	1.28
23-2 86-90	338.36	17.75	1.50	1.11
23-3 87-91	339.87	17.81	1.57	1.12
23-4 92-96	341.42	17.87	1.56	0.90
23-4 141-145	341.91	17.89	1.46	0.71
24-1 105-109	356.05	21.62	1.73	0.94
24-1 140-144	356.40	21.66	1.42	0.81
24-2 31-35	356.81	21.70	1.32	1.01
25-1 91-95	374.91	23.64	1.66	0.91
25-2 70-74	376.20	23.78	1.76	1.05
26-2 85-89	394.25	24.21	1.68	1.18
27-1 96-100	412.96	24.65	1.30	0.91
27-2 75-79	414.25	24.68	1.27	0.90
27-3 87-91	415.87	24.71	1.20	1.03
27-4 88-92	417.38	24.75	1.17	0.85
28-1 103-107	432.03	25.10	1.69	0.85
		Site 553		
3-1 50-54	151.50	5.38	2.15	0.77
3-1 142-146	152.42	5.42	2.26	0.84
3-2 50-54	153.00	5.45	2.26	0.74
3-3 50-54	154.50	5.52	2.18	0.76
3-3 118-122	155.18	5.54	2.34	0.64
3-4 118-122	156.68	5.60	2.27	0.75
3-4 140-144	156.90	5.62	2.25	0.85
3-5 52-56	157.52	5.67	2.12	0.60
3-5 110-114	158.10	5.72	2.28	0.57
3-6 52-56	159.02	5.80	2.22	0.63
3-6 118-122	159.68	5.85	2.31	0.85
4-1 85-89	180.35	7.57	1.99	1.18
4-1 130-134	180.80	7.60	2.08	1.32
4-2 75-79	181.75	7.68	2.26	1.31
4-2 140-144	182.40	7.74	2.14	1.10
4-3 50-54	183.00	7.79	2.16	1.48
4-3 136-140	183.86	7.86	2.19	1.25
4-4 82-86	184.82	7.94	2.18	1.28
4-4 130-134	185.30	7.98	2.10	1.28
4-5 30-34	185.80	8.02	2.12	1.31
4-5 90-94	186.40	8.07	2.09	1.44
4-6 30-34	187.30	8.29	2.07	1.16
4-6 80-84	187.80	8.41	2.19	1.28
4-6 130-134	188.30	8.53	2.34	1.26
4-7 24-28	188.74	8.63	2.22	1.02
5-1 31-35	189.31	8.77	2.00	0.93
5-1 31-35	189.31	8.77	2.06	0.94
5-1 100-104	190.00	8.86	2.16	0.99
5-2 11-15	190.61	8.95	2.11	1.12
5-2 20-24	191.20	9.03	2.10	1.10
5-2 117-121	191.67	9.09	1.99	1.03
5-3 24-28	192.24	9.17	2.06	1.08
5-3 100-104	193.00	9.27	2.22	0.94
5-4 14-18	193.64	9.36	1.99	1.07
5-4 80-84	194.30	9.44	2.05	0.96
5-5 19-23	195.19	9.56	1.96	1.04
5-5 81-85	195.81	9.65	2.13	0.98
5-6 70-74	197.20	9.84	2.03	0.99
5-6 80-84	197.30	9.85	2.29	0.88
6-1 56-60	199.06	10.05	2.25	1.04
6-1 133.137	199.83	10.14	1.96	1.16
6-2 14-18	200.14	10.18	2.08	1.18
6-2 70-74	200.70	10.24	2.13	1.15
6-2 82-86	200.82	10.26	1.91	1.06
6-3 17-21	201.67	10.36	1.91	1.02
6-3 82-86	202.32	10.43	2.06	0.99
6-4 8-12	203.08	10.54	2.01	1.12
6-5 23-27	204.73	10.71	1.94	1.00
6-5 70-74	205.20	10.76	2.03	0.96
6-5 133-137	205.83	10.84	2.02	1.11
6-6 23-27	206.23	10.88	2.01	1.01
7-1 14-18	208.14	11.10	2.07	1.18
7-1 80-84	208.80	11.18	2.10	1.04
7-1 126-130	209.26	11.27	1.88	1.12
7-2 25-29	209.75	11.36	1.92	1.11
7-2 80-84	210.30	11.47	2.04	1.05
7-2 100-104	210.50	11.51	1.86	1.08
7-3 24-28	211.24	11.65	1.90	0.92
7-3 80-84	211.80	11.76	2.09	0.97
7-3 125-129	212.25	11.85	1.91	1.06
7-4 25-29	212.75	11.94	1.83	1.05
7-4 80-84	213.30	12.05	1.80	1.03
7-4 80-84	213.50	12.09	1.90	1.00
7-4 128-132	213.78	12.14	1.72	1.01
7-5 130-134	214.30	12.24	1.82	0.94
7-5 130-134	215.30	12.44	1.87	0.92
7-6 25-29	215.75	12.52	1.86	1.17
7-6 80-84	216.30	12.63	1.91	1.18

TABLE 3. (continued)

Sample	Depth	Age	$\delta^{18}O$	$\delta^{13}C$
8-1 16-20	217.66	12.82	1.69	1.21
8-1 80-84	218.30	12.91	2.01	1.13
8-1 135-139	218.85	12.99	1.65	1.18
8-2 38-42	219.38	13.06	1.47	1.25
8-3 24-28	220.03	13.32	1.90	1.58
8-3 24-28	220.74	13.59	1.69	1.43
8-3 49-53	220.99	13.69	1.96	1.30
8-3.77-81	221.77	14.00	1.48	0.98
9-1 57-61	227.57	22.65	1.26	0.77
9-1 118-122	228.18	22.75	1.13	0.88
9-2 26-30	228.76	22.87	1.19	0.76
9-2 95	229.45	23.07	1.24	0.65
9-3 25-29	230.25	23.31	1.13	0.66
9-3 80-84	230.80	23.47	0.96	0.60
9-3 141-145	231.41	23.64	1.17	0.63
9-4 16-20	231.66	23.72	1.13	0.60
9-4 70-74	232.20	23.87	1.16	0.77
9-5 61-65	233.61	24.29	1.37	0.63
9-5 105-109	234.05	24.41	0.95	0.61
9-6 40-44	234.90	24.66	0.19	0.17
	Site 555			
5-5 100	41.00	5.67	1.86	0.59
6-5 100	52.00	6.11	2.33	0.80
7-5 14	59.14	6.40	2.34	0.74
8-1 108	63.58	6.58	2.19	1.06
8-3 108	66.58	6.70	2.32	0.93
8-5 108	69.58	6.82	1.99	1.15
8-5 108	69.58	6.82	2.18	1.01
8-5 108	69.58	6.82	2.10	0.87
9-1 55	91.55	7.71	2.11	1.23
9-2 103	93.53	7.79	2.30	1.14
10-1 110	101.60	8.12	2.26	1.28
10-3 100	104.50	8.24	2.09	1.14
10-5 90	107.40	8.35	2.12	1.15
11-1 100	130.00	9.27	2.07	1.11
11-3 106	133.06	9.39	2.08	1.29
12-1 143	139.93	9.67	1.76	0.90
12-2 109	141.09	9.72	1.94	1.06
13-1 19	148.19	10.00	2.01	1.06
14-1 31	157.81	10.39	1.96	0.91
15-1 124	168.24	10.82	1.99	1.40
16-3 124	180.90	11.33	1.96	0.85
16-4 110	182.10	11.38	1.94	0.86
16-5 110	183.60	11.44	1.83	0.88
16-6 80	184.80	11.49	1.91	0.89
16-7 21	185.71	11.52	2.11	1.02
17-1 130	187.30	11.59	2.08	0.81
17-1 130	187.30	11.59	2.00	0.82
17-2 120	188.70	11.64	1.97	0.94
17-3 110	190.10	11.70	1.92	0.78
17-4 13	190.63	11.72	2.06	0.53
18-1 133	196.83	11.97	1.92	1.02
18-2 83	197.83	12.01	1.88	0.96
19-1 118	206.18	12.35	2.02	1.00
19-2 114	207.64	12.41	1.98	1.18

TABLE 3. (continued)

Sample	Depth	Age	$\delta^{18}O$	$\delta^{13}C$
19-3 18	208.18	12.43	1.99	1.21
20-1 101	215.51	12.73	1.91	1.01
20-2 114	217.14	12.79	2.00	0.98
21-1 130	225.30	13.12	1.92	0.97
21-2 110	226.60	13.18	1.92	1.09
22-1 107	234.57	13.50	1.45	1.10
22-2 20	235.20	13.52	1.18	1.15
23cc	243.01	13.87	2.11	0.47
23cc	243.01	13.87	2.11	0.69
24-1 70	253.20	14.25	1.42	0.92
24-2 120	255.20	14.33	0.93	0.64
24-3 120	256.70	14.39	1.26	1.21
24-4 110	258.10	14.46	1.19	0.81
24-5 55	259.05	17.41	1.04	0.82
23cc	243.01	17.62	2.11	0.47
23cc	243.01	17.62	2.11	0.69
25-3 91	265.91	17.90	1.32	0.83
25-4 118	267.68	18.03	0.88	0.92
25-5 125	269.25	18.15	0.75	0.89
25-6 105	270.55	18.24	0.69	0.89
26-1 76	272.26	18.37	1.07	0.93
26-1 76	272.26	18.37	1.15	0.88
26-2 70	273.70	18.47	0.90	0.93
26-2 70	273.70	18.47	0.93	1.03
26-3 102	275.52	18.60	0.83	0.59
26-4 55	276.55	18.68	0.88	0.23
26-5 100	278.50	18.82	0.83	0.68
26-6 132	280.32	18.95	0.68	0.88
	Site 563			
4-3 40-44	189.90	10.55	1.80	0.91
5-1 30-34	194.80	10.90	1.84	1.11
5-1 115-119	195.65	10.96	1.93	1.15
5-1 135-139	195.85	10.97	1.87	1.21
5-2 50-54	196.50	11.02	1.89	1.16
5-3 45-49	197.95	11.12	2.00	1.36
5-3 115-119	198.65	11.17	2.02	1.42
5-3 135-139	198.85	11.19	2.02	1.37
5-4 34-38	199.34	11.22	2.06	1.48
5-4 110-114	200.10	11.27	1.64	1.21
5-4 134-138	200.34	11.29	1.84	1.57
5-5 50-54	201.00	11.34	1.92	1.16
5-6 30-34	202.30	11.43	1.89	1.49
5-6 110-114	203.10	11.49	1.82	1.04
5-6 138-142	203.38	11.51	1.69	0.82
5-7 30-34	203.80	11.54	1.59	1.03
6-1 30-34	204.30	11.57	1.71	0.94
6-1 105-109	205.05	11.61	1.76	0.89
6-2 50-54	206.00	11.66	1.74	0.46
6-3 34-38	207.34	11.73	1.63	0.91
6-3 110-114	208.10	11.77	1.66	0.75
6-4 30-34	208.80	11.81	1.82	0.77
6-4 110-114	209.60	11.86	1.91	0.95
6-7 17-21	210.17	11.89	1.79	1.00
6-5 46-50	210.46	11.90	1.84	0.90
6-6 30-34	211.80	11.97	1.74	0.80

TABLE 3. (continued)

Sample	Depth	Age	$\delta^{18}O$	$\delta^{13}C$
	Site 563			
7-1 35-39	213.85	12.09	2.03	1.04
7-2 118-122	216.18	12.21	2.00	1.15
7-3 35-39	216.85	12.25	2.04	1.10
7-3 110-114	217.60	12.29	2.03	1.15
7-4 30-34	218.30	12.33	1.85	1.01
7-4 110-114	219.10	12.37	2.11	1.10
7-5 30-34	219.80	12.41	2.03	1.01
7-6 30-34	221.30	12.49	1.90	0.98
7-6 110-114	222.10	12.54	2.06	1.03
7-7 30-34	222.80	12.57	2.11	0.72
8-1 34-38	223.34	12.60	1.98	1.09
8-1 120-124	224.20	12.65	1.96	1.09
8-2 40-44	224.90	12.69	1.97	0.99
8-3 40-44	226.40	12.77	1.59	0.84
8-3 120-124	227.20	12.81	1.48	1.03
8-4 30-34	227.80	12.86	1.36	0.92
8-4 120-124	228.70	12.94	1.59	1.05
8-5 25-29	229.25	12.99	1.48	1.10
8-6 28-32	230.78	13.13	1.81	1.25
8-6 114-118	231.64	13.21	1.51	1.28
8-7 20-24	232.20	13.26	1.52	0.74
9-1 100-104	233.50	13.38	1.63	1.61
9-3 10-14	235.60	13.58	1.63	1.39
9-4 25-29	237.25	14.83	1.14	0.98
9-5 33-37	238.83	14.99	1.31	1.26
9-6 33-37	240.33	15.15	1.17	1.32
9-7 33-37	241.83	15.30	1.03	1.51
10-1 33-37	242.33	15.35	1.02	1.55
10-2 18-22	243.68	15.49	1.01	1.52
10-3 23-27	245.23	15.64	1.04	1.74
10-4 23-27	246.73	15.79	1.29	2.00
10-5 16-20	248.16	15.94	1.29	1.78
10-6 13-17	249.63	16.08	1.29	1.47
10-7 17-21	251.27	16.27	1.24	1.51
11-1 17-21	251.67	16.33	1.24	1.95
11-2 32-36	253.32	16.61	1.14	1.85
11-3 19-23	254.69	16.84	0.72	1.46
11-4 25-29	255.25	16.93	0.81	1.32
11-5 9-13	257.59	17.25	1.27	1.18
12-1 35-39	261.35	17.69	1.16	1.16
12-1 113-117	262.13	17.76	1.13	1.18
12-2 23-27	262.73	17.80	0.95	1.26
12-3 39-43	264.39	17.95	1.52	1.01
12-4 12-4 44-48	265.94	18.09	1.31	1.05
12-4 116-120	266.66	18.16	1.16	0.86
12-5 38-42	267.38	18.26	1.45	1.15
12-6 30-34	268.80	18.46	1.46	0.98
12-7 10-14	270.10	18.60	1.27	0.95
13-1 121-125	271.71	18.71	1.21	0.67
13-2 48-52	272.48	18.77	1.29	0.59
13-3 79-53	273.99	18.87	1.29	0.48
13-4 21-25	275.21	18.96	1.48	0.69
13-4 100-104	276.00	20.77	1.22	1.07
13-5 42-46	276.92	20.94	1.37	0.95
14-1 53-57	280.53	21.61	1.67	1.06
14-1 126-131	281.26	21.72	1.68	0.89

TABLE 3. (continued)

Sample	Depth	Age	$\delta^{18}O$	$\delta^{13}C$
14-2 46-50	281.96	21.78	1.67	0.95
14-3 141-145	284.41	21.99	1.34	0.79
14-5 30-34	287.30	22.23	1.38	0.68
14-6 138-142	288.88	22.37	1.69	1.00
15-1 50-54	290.00	22.46	1.18	0.92
15-1 124-128	290.74	22.52	1.33	1.30
15-2 45-49	291.45	22.59	1.20	1.09
15-3 51-55	293.01	22.78	1.46	1.10
15-3 120-124	293.70	22.87	1.60	1.39
15-4 44-48	294.44	22.96	1.45	1.42
15-5 31-35	295.81	23.11	1.51	1.36
15-6 23-27	297.23	23.26	1.54	1.11
15-7 20-24	298.70	23.42	1.38	0.71
16-1 30-34	299.30	23.49	1.39	0.91
16-2 37-41	300.87	23.66	1.66	1.32
16-3 35-39	302.35	23.84	2.03	1.32
16-4 38-42	303.88	24.22	1.63	1.25
	Site 608			
27-2 87-91	245.27	10.61	2.20	0.85
27-4 86-90	248.36	10.77	2.08	1.03
27-7 11-15	252.01	10.96	2.20	1.35
28-1 90-94	253.40	11.03	2.19	0.83
28-1 90-94	253.40	11.03	2.22	0.81
28-2 17-21	254.17	11.07	2.16	1.10
28-3 23-27	255.73	11.15	2.23	0.69
28-5 17-21	258.67	11.29	2.13	0.61
29-1 127-131	263.37	11.53	1.91	1.08
29-3 64-68	265.74	11.67	2.07	0.96
29-5 50-54	268.60	11.84	1.95	1.05
30-1 128-132	272.98	12.09	2.06	1.13
30-3 15-19	274.85	12.20	2.00	1.12
30-5 22-26	277.92	12.38	2.05	0.99
31-1 85-89	282.15	12.63	2.22	0.96
31-2 75-79	283.55	12.71	2.17	1.13
31-4 21-25	286.01	12.85	1.75	1.17
31-6 52-56	289.32	13.00	1.48	1.23
32-1 80-84	291.70	13.11	1.70	1.32
32-5 80-84	297.70	13.53	1.74	1.74
33-2 47-51	302.47	13.88	1.43	1.38
33-3 29-33	303.79	13.97	1.16	1.42
33cc	304.30	14.01	1.19	1.67
34-2 109-113	313.69	14.66	0.98	1.68
34-4 105-109	315.65	14.80	1.07	1.12
34-6 110-114	318.70	15.01	0.86	1.23
35-1 110-114	320.80	15.16	1.15	1.09
35-3 115-119	323.85	15.40	1.28	1.65
35-5 97-101	326.67	15.67	1.27	1.48
36-1 90-94	330.20	16.00	1.42	1.84
36-2 60-64	331.40	16.12	1.46	1.99
36-3 92-96	333.22	16.30	1.05	1.92
36-4 33-37	334.13	16.40	1.20	1.42
36-5 100-104	336.30	16.64	0.93	1.57
36-6 34-38	337.14	16.73	0.84	1.42
37-1 111-115	340.01	17.05	0.81	1.23
37-1 111-115	340.01	17.05	0.65	1.11

TABLE 3. (continued)

Sample	Depth	Age	$\delta^{18}O$	$\delta^{13}C$
37-2 89-93	341.29	17.19	0.96	1.13
37-3 100-104	342.90	17.37	1.16	1.40
37-3 100-104	342.90	17.37	0.92	1.17
37-4 70-74	344.10	17.51	1.22	1.13
37-5 110-114	346.00	17.71	1.49	1.02
37-5 110-114	346.00	17.71	1.31	1.04
37-6 78-82	347.18	17.84	1.40	1.09
38-1 66-70	349.16	18.05	1.59	0.85
38-1 66-70	349.16	18.05	1.52	0.96
38-2 33-37	350.33	18.17	1.26	0.88
38-3 69-73	352.19	18.37	1.17	0.88
38-3 69-73	352.19	18.37	1.04	0.84
38-4 60-64	353.60	18.52	1.25	0.87
38-5 73-77	355.23	18.68	1.28	0.76
39-1 70-74	358.80	19.00	1.43	0.87
39-3 17-21	361.27	19.22	1.17	0.54
39-3 17-21	361.27	19.22	1.03	0.45
39cc	364.27	19.48	1.24	0.86
40-2 85-89	370.05	19.99	1.25	0.41
40-4 117-121	373.37	20.27	1.24	0.82
40cc	376.01	20.50	1.51	0.87
41-2 92-96	379.82	21.78	1.53	0.87
41-4 107-112	382.87	22.00	1.30	0.58
41-6 86-90	385.26	22.18	1.14	0.52
42-1 100-104	387.90	22.37	1.06	0.99
42-3 100-105	390.90	22.58	1.19	0.71
42-5 86-90	393.76	22.69	1.34	0.74
43-1 115-119	397.65	22.85	1.41	1.42
43-3 110-114	400.60	22.97	1.13	1.12
43-3 110-114	400.60	22.97	1.10	0.96
43-5 10-14	402.60	23.05	1.49	0.99
44-2 10-14	407.70	23.25	1.50	1.44
44-4 7-11	410.67	23.47	1.46	1.17
44cc	411.36	23.53	1.70	1.40
44cc	411.36	23.53	1.56	1.36
45-1 38-42	416.08	23.91	1.20	1.33
45-4 38-42	420.58	24.28	1.07	0.83
45-5 38-42	422.08	24.40	0.96	0.82
45-6 38-42	423.58	24.52	1.06	0.71
46-1 38-42	425.68	24.70	0.97	0.73
46-2 38-42	427.18	24.82	1.09	0.80
46-3 24-28	428.68	24.94	1.11	0.60
46-4 21-25	430.01	25.05	1.51	0.78
	Site 704			
47-3 44-48	435.64	16.35	1.18	1.57
47-5 44-48	438.64	16.72	0.93	1.20
47-6 44-48	440.14	16.79	1.27	1.31
47cc	441.50	16.85	0.99	1.28
48-1 59-63	442.29	16.88	1.18	1.16
48-2 59-63	443.79	16.95	1.12	1.20
48-3 59-63	445.29	17.01	1.38	1.37
48cc	446.20	17.05	1.41	1.51
49-2 30-34	453.00	17.36	1.09	1.25
49-4 30-34	456.00	17.46	1.09	1.19
50-1 19-23	460.89	17.61	1.18	0.74

TABLE 3. (continued)

Sample	Depth	Age	$\delta^{18}O$	$\delta^{13}C$
51-1 130-134	464.00	17.71	1.42	1.02
52-2 50-54	474.20	18.03	1.63	0.57
52-4 50-54	477.20	18.15	1.23	0.58
53-1 20-24	481.90	18.36	1.38	0.79
53-3 20-24	484.90	18.50	1.53	0.70
54-1 140-144	492.60	18.85	1.39	0.29
54-2 140-144	494.10	18.92	1.50	0.40
54-3 140-144	495.60	18.99	1.12	0.21
54-5 110-114	498.30	19.11	1.16	0.48
54-6 140-144	500.10	19.20	1.46	0.44
54cc	500.35	19.21	1.45	0.50
55-1 90-94	501.60	19.26	1.21	0.87
55-1 90-94	501.60	19.26	1.25	0.96
55-2 90-94	503.10	19.33	1.53	1.07
55-2 90-94	503.10	19.33	1.54	1.15
55-3 90-94	504.60	19.40	1.41	0.85
55-4 90-94	506.10	19.47	1.34	0.60
55-5 90-94	507.60	19.54	1.61	0.66
55-6 90-94	509.10	19.61	1.50	0.54
55cc	509.85	19.64	1.47	0.39
56-1 100-104	511.20	19.78	1.29	0.72
56-2 100-104	512.70	19.93	1.28	0.46
56-3 100-104	514.20	20.09	1.47	0.53
56-4 100-104	515.70	20.24	1.30	0.56
57-1 37-41	520.07	20.39	1.56	0.92
57cc	528.85	20.70	1.60	0.75
58-1 106-110	530.26	20.75	1.69	0.61
58-2 106-110	531.76	20.81	1.42	0.64
58-2 106-110	531.76	20.81	1.46	0.76
58-3 106-110	533.26	20.86	1.72	0.82
58-4 106-110	534.76	20.95	1.53	0.60
58-5 106-110	536.26	21.03	2.08	0.64
58-6 106-110	537.76	21.12	1.59	0.76
58cc	539.05	21.19	1.41	0.66
59-1 136-140	540.06	21.25	1.38	0.85
59-2 136-140	541.56	21.34	1.53	0.97
59-3 136-140	543.06	21.42	1.36	0.67
59-4 136-140	544.56	21.51	1.47	0.80
60-1 36-40	548.56	21.74	1.49	0.97
60-6 36-40	556.06	22.17	1.65	0.75
61-1 90-94	558.60	22.35	1.30	0.66
61-2 90-94	560.10	22.46	1.40	0.67
62-1 100-104	568.20	22.97	1.58	1.22
62-1 100-104	568.20	23.05	1.31	1.17
62-2 100-104	569.70	23.16	1.59	1.53
62-4 100-104	572.70	23.37	1.48	1.31
62-5 100-104	574.20	23.48	1.42	0.90
62cc	575.85	23.59	1.54	1.19
63-1 47-51	577.17	23.68	1.44	1.36
63-2 47-51	578.67	23.78	2.32	1.86
63-3 47-51	580.17	23.88	1.95	1.75
63-4 47-51	581.67	24.01	1.82	1.29
63-5 47-51	584.17	24.23	1.46	1.15
63-6 15-19	584.35	24.24	1.57	1.05
64-1 50-54	586.70	24.45	1.35	0.85
64-2 50-54	588.20	24.58	1.48	1.12
64-3 50-54	589.70	24.71	1.68	1.07

TABLE 3. (continued)

Sample	Depth	Age	$\delta^{18}O$	$\delta^{13}C$
64cc	590.15	24.75	1.15	0.87
65-1 75-79	596.45	25.30	1.36	1.02
65-2 75-79	597.95	25.43	1.24	0.98
65-3 72-77	599.43	25.56	1.32	0.75

northern North Atlantic; or (2) the Greenland-Scotland Ridge was an effective barrier to dense water overflowing into the North Atlantic [Vogt, 1972; Schnitker, 1980; Blanc et al., 1980]. In either case, the North Atlantic was relegated to a passive role in the earliest Miocene. This situation is strikingly different from the modern ocean but analogous to the early Paleogene oceans when the highest $\delta^{13}C$ values were recorded in the Southern Ocean [Miller et al., 1987]. The Pacific and Indian reconstructions have too few data to interpret, and the role of WSDW from the Tethys cannot be evaluated.

The early Miocene (Zone Mi1b, 18.3 Ma). The high $\delta^{13}C$ signature of NCW was evident at 18.3 Ma (Figure 12), in contrast to the earliest Miocene (23.6 Ma). In addition to the North Atlantic, high $\delta^{13}C$ values were recorded in the southern hemisphere intermediate waters, while the lowest $\delta^{13}C$ values were recorded in the North Pacific (Figure 12). The deepwater $\delta^{13}C$ patterns indicate that the North Atlantic was a source for deep water and the North Pacific was the "end-of-the-line" for deepwater circulation.

An intermediate water mass with a high $\delta^{13}C$ signal was prominent in the southern hemisphere of the Indian and Pacific oceans (Figure 12). Coverage of the South Atlantic is insufficient to record this $\delta^{13}C$ signal. (However, intervals with better coverage show a high $\delta^{13}C$ signal in the South Atlantic as well.) Two possible sources for a high $\delta^{13}C$ intermediate water mass follow:

1. Woodruff and Savin [1989] proposed that the high $\delta^{13}C$ values at intermediate to upper deep water depths originated in the northern Indian Ocean with the production of a warm, saline water mass. This water mass may have flowed into the Southern Ocean, where it was redistributed into the Pacific and

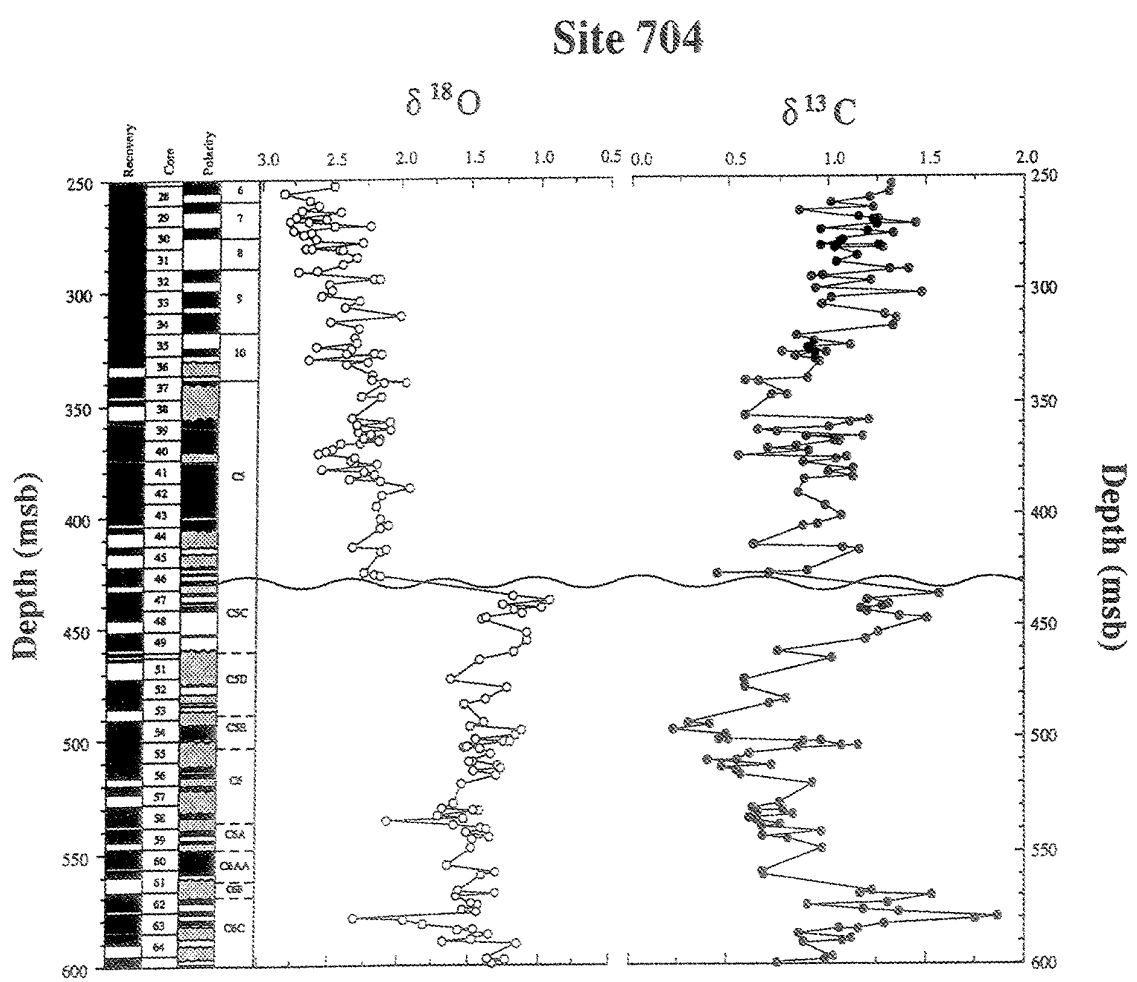

Fig. 7. Site 704 (Meteor Rise) $\delta^{18}O$ and $\delta^{13}C$ isotope data plotted versus depth.

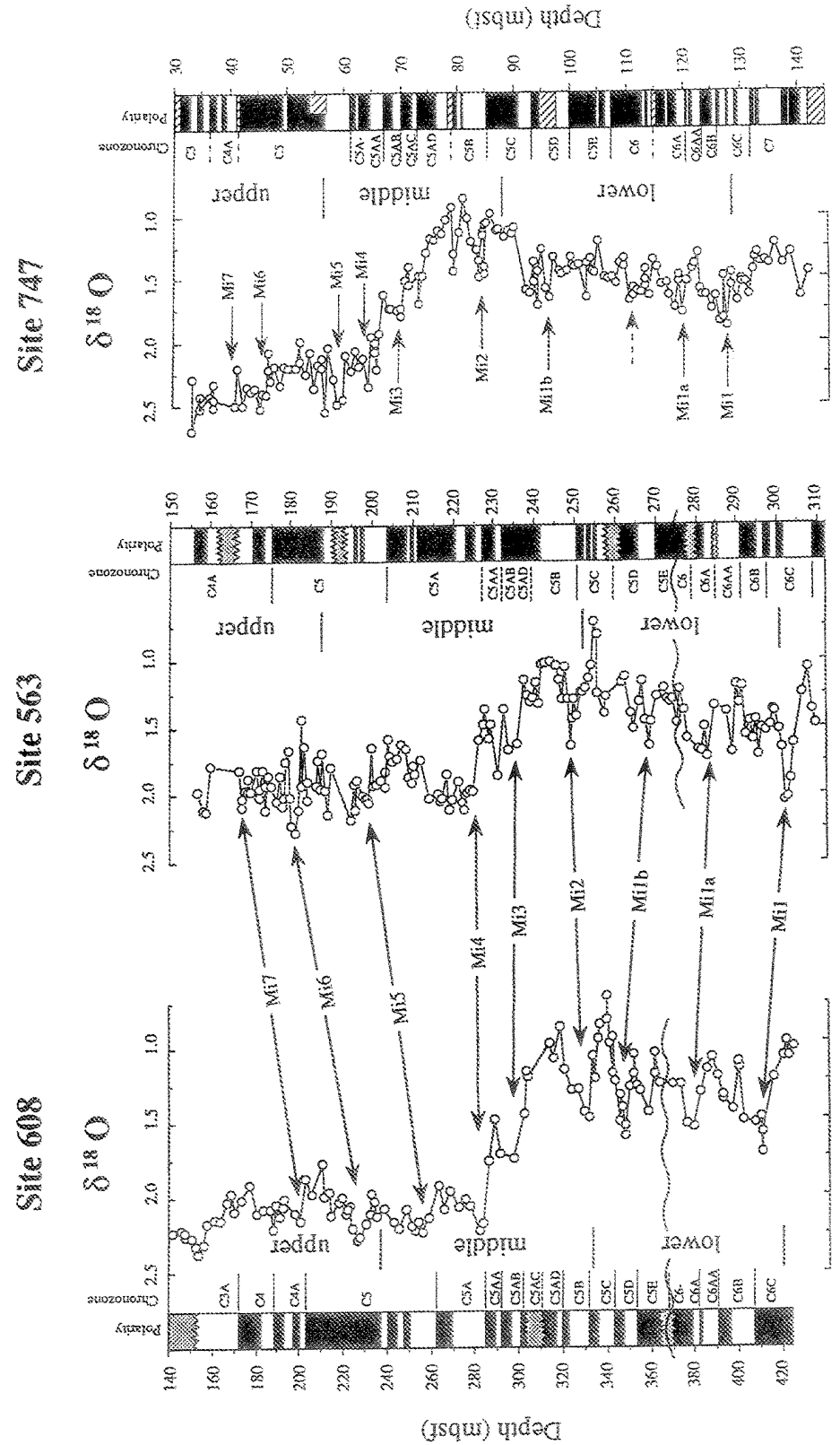

Fig. 8. $\delta^{18}O$ records from Sites 563, 608, and 747, marking "Mi" events and their correlation to the Geomagnetic Polarity Time Scale.

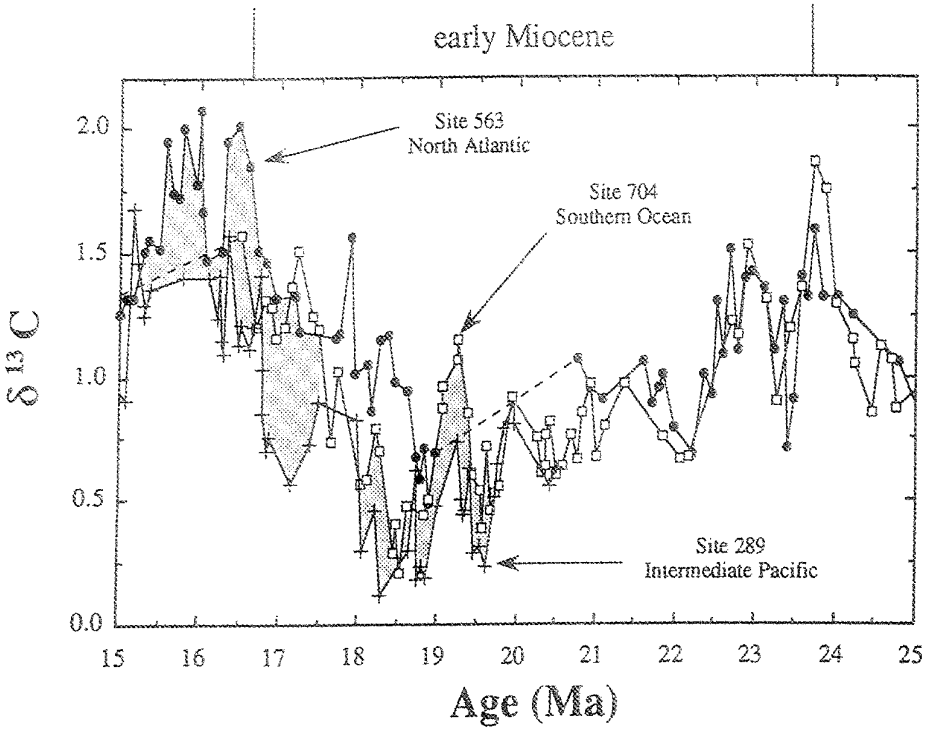

Fig. 9. Early Miocene $\delta^{13}C$ time series records from Sites 563 (North Atlantic, solid circles), 289 (intermediate Pacific, pluses), and 704 (Southern Ocean, boxes). Note the periodic separation between all three $\delta^{13}C$ records from ~20 to 16 Ma, when the North Atlantic recorded the highest values and the Pacific recorded the lowest values. Intervals during which Southern Ocean $\delta^{13}C$ values were higher than those in the Pacific must represent the contribution of another water mass with a high $\delta^{13}C$ signal to elevate the Southern Ocean over the Pacific value. From 20 to 16 Ma, high North Atlantic $\delta^{13}C$ values identify the North Atlantic as at least one source.

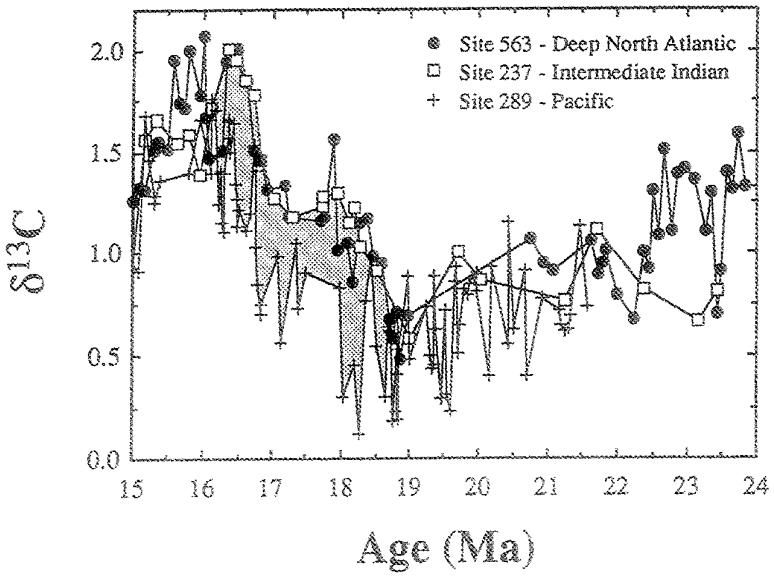

Fig. 10. Early Miocene $\delta^{13}C$ time series records from Sites 563 (North Atlantic, solid circles), 237 (intermediate equatorial Indian, pluses; data from Woodruff and Savin [1991]), and 704 (Southern Ocean, boxes). Note the similarity between the North Atlantic and Indian Ocean records from ~20 to 16 Ma. As in Figure 9, high $\delta^{13}C$ values in the Indian Ocean indicate that it was near a source of high $\delta^{13}C$ water to the Southern Ocean.

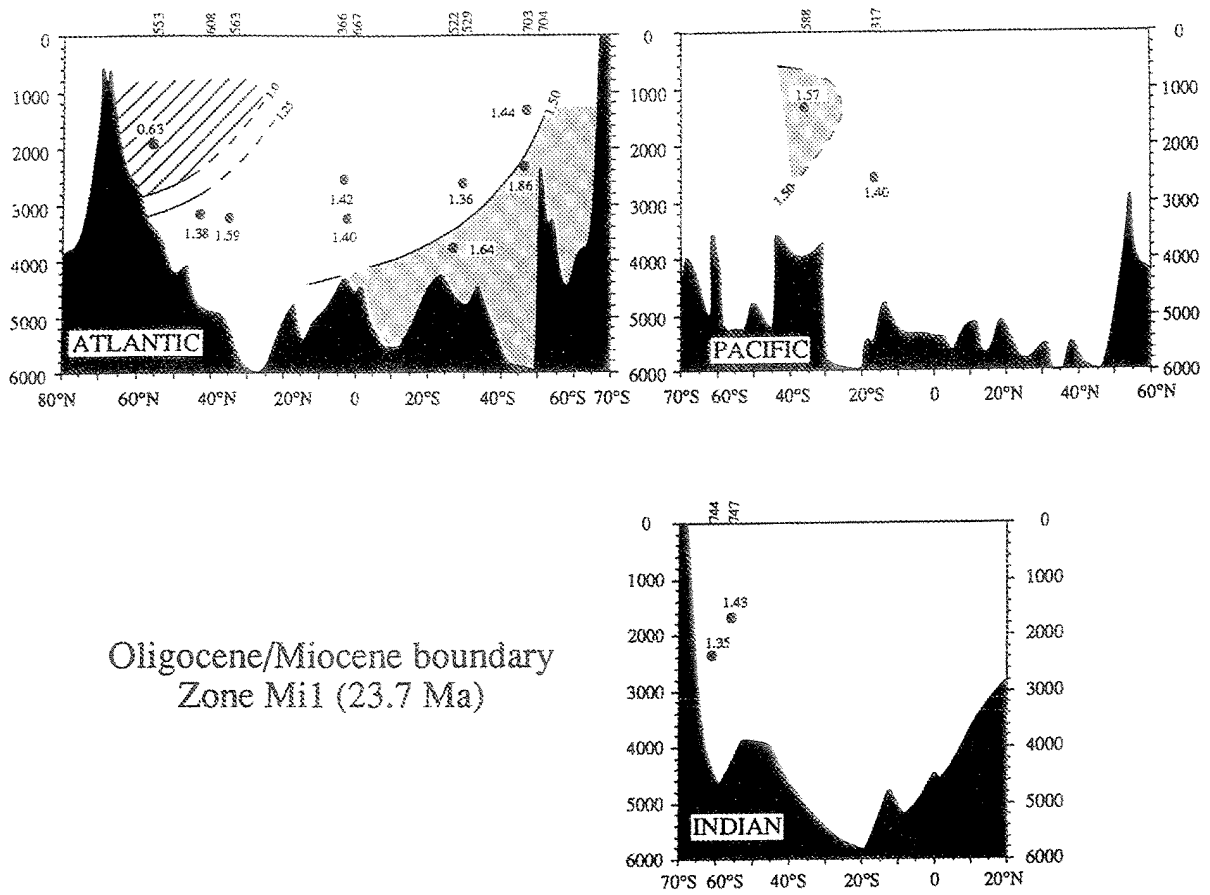

Fig. 11. Earliest Miocene (Zone Mi1 - 23.7 Ma) time slice reconstruction showing a south to north $\delta^{13}C$ gradient in the Atlantic Ocean. The South Atlantic recorded the highest $\delta^{13}C$ values with a low $\delta^{13}C$ water mass in the intermediate North Atlantic. This pattern can only represent a single source deepwater circulation system. The low $\delta^{13}C$ values recorded on the Rockall Plateau (Site 553) indicate the lack of NCW production. Data for this reconstruction are in Table 2a.

Atlantic oceans. The high $\delta^{13}C$ value recorded at Indian Ocean Site 237 is consistent with production of a Tethyan water mass (Figure 12). In support of this argument, the eastern Tethys produced evaporitive sequences during the late early and middle Miocene, which may be indicative of restricted or semirestricted basins [Richardson and Arthur, 1988]. (However, the most extensive evaporite sequences were deposited in the middle and late Miocene [Richardson and Arthur, 1988], after the lowest $\delta^{18}O$ values were recorded.) Warm, salty water masses may have formed in these basins and flowed into the Indian Ocean to form WSDW [Woodruff and Savin, 1989]. However, it is more difficult to account for the high values in the intermediate South Atlantic and South Pacific oceans with this mechanism. Nevertheless, we concur with Woodruff and Savin [1989] that the production of a Tethyan water mass may have been tied to the destruction of the Tethys. Therefore the 5 to 10 m.y. period immediately preceding 15 Ma may have been the most conducive for WSDW production in this region, given this rough estimate for the termination of the eastern Tethys.

2. The Southern Ocean is a logical source for the high $\delta^{13}C$ values observed at intermediate depths because they are recorded in the Atlantic and Pacific oceans as well as in the Indian Ocean. This water mass would be analogous to AAIW, but with a more distinct $\delta^{13}C$ signature. We term this intermediate water mass as Southern Component Intermediate Water (SCIW), which may have originated in the Southern Ocean.

It is not unexpected for upper CPW to have a high $\delta^{13}C$ signature. Charles and Fairbanks [1990] demonstrated that air-sea interactions enrich the $\delta^{13}C$ value of Antarctic Intermediate Water (AAIW) source waters by approximately 1‰ over the expected value. The high nutrient levels and the remineralization of organic matter associated with the high productivity in today's Southern Ocean obscured detection of the signal in the modern ocean until recently [Charles and Fairbanks, 1992]. This effect may have been accentuated at times when mean ocean nutrient levels were low, such as during the early and middle Miocene [Delaney, 1990] or when the residence time of water at the surface was lengthened. In

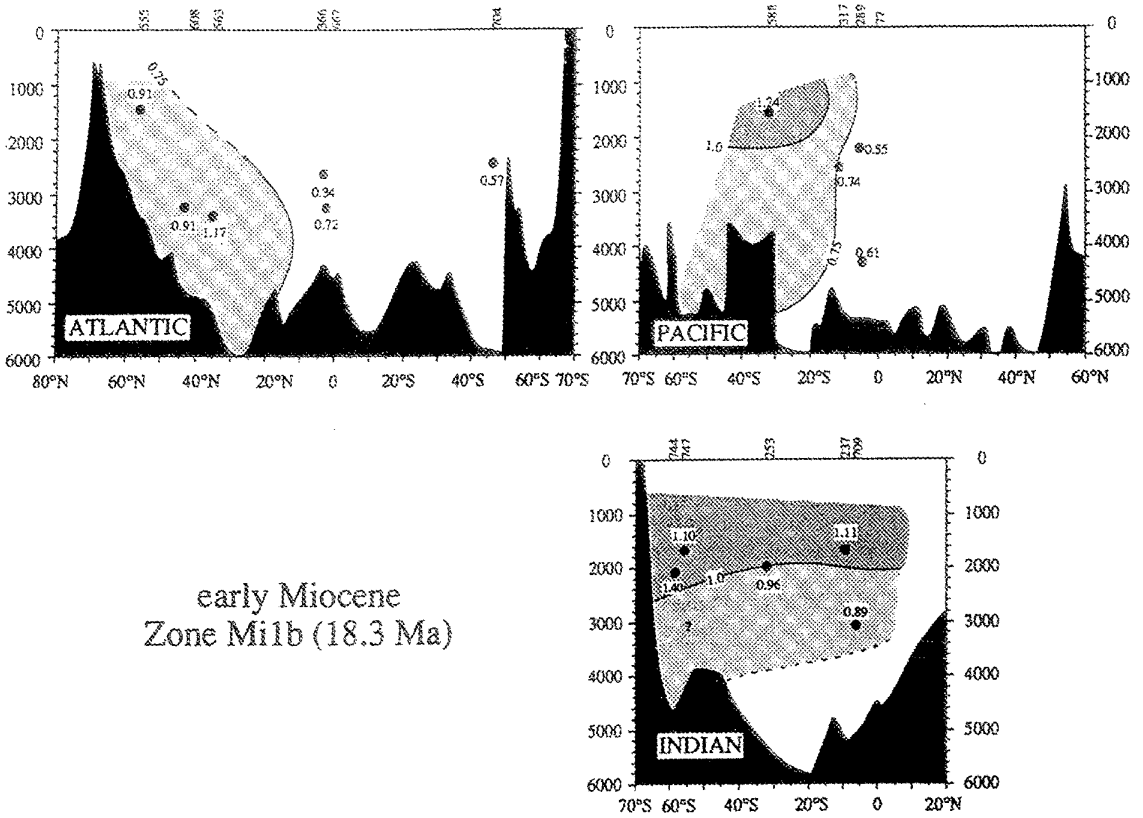

Fig. 12. Early Miocene (Zone Mi1b - 18.3 Ma) time slice reconstruction showing a moderate north to south $\delta^{13}C$ gradient in the Atlantic Ocean which is in contrast to the earliest Miocene gradient (Figure 11). The North Atlantic and intermediate Indian Ocean recorded the highest $\delta^{13}C$ values with the lowest $\delta^{13}C$ water mass in the intermediate North Pacific. This pattern represents a three-component ocean where SCW production was supplemented by the production of two water masses with a "young" or high $\delta^{13}C$ signal. There is evidence in this figure that a high $\delta^{13}C$ water mass originated in the Southern Ocean and spread to the north at intermediate depths. Data for this reconstruction are in Table 2b.

support of low mean oceanic nutrient levels, Delaney [1990] used Cd/Ca ratios from Site 289 and South Atlantic Site 525 to conclude that the Cd inventory, and hence the phosphorous inventory was approximately 80% of the modern level during the early and middle Miocene. Wright et al. [1991] speculated that middle and early late Miocene nutrient levels were only one half to two thirds of the modern level based on lower surface to deep $\delta^{13}C$ differences. Therefore the $\delta^{13}C$ enrichment of AAIW through air-sea exchange may have been better expressed in the early and middle Miocene than in the modern oceans, because of lower mean ocean nutrient levels (Figure 12).

The intermediate water signal in the Indian Ocean is still problematic. As documented in the South Atlantic and Pacific, the $\delta^{13}C$ signature of SCIW is very pronounced and may account for the high intermediate Indian Ocean values. However, the penetration of this signal to the equatorial regions in the Indian Ocean may require a compensating flow to the south at greater depths. This situation would be analogous to the modern South Atlantic where AAIW is drawn to the north across the equatorial regions as part of the water returning to the North Atlantic to replace NADW [Gordon and Piola, 1983; Broecker et al., 1988]. Alternatively, the high $\delta^{13}C$ values in the equatorial Indian Ocean in the early Miocene may represent the Tethyan water signal, which is indistinguishable from SCIW. In either case, the high $\delta^{13}C$ values at Site 237 may reflect the production of a deep to intermediate water mass in the northern Indian Ocean, whether as a direct measure of Tethyan water or as a consequence of Tethyan outflow.

The early/middle Miocene boundary (Zone Mi2 - 16.2 Ma). Northern Component Water continued to be an important deepwater source through the end of the earliest middle Miocene (16.2 Ma). If we focus on the deep ocean, a clear pattern emerges. The highest $\delta^{13}C$ values were in the North Atlantic, the lowest values were in the North Pacific, and intermediate values in the Southern Ocean (Figure 13). This pattern is similar to the present except that the absolute values differed. This difference is accounted for by differences in the mean ocean $\delta^{13}C$ value. Intermediate water from the southern

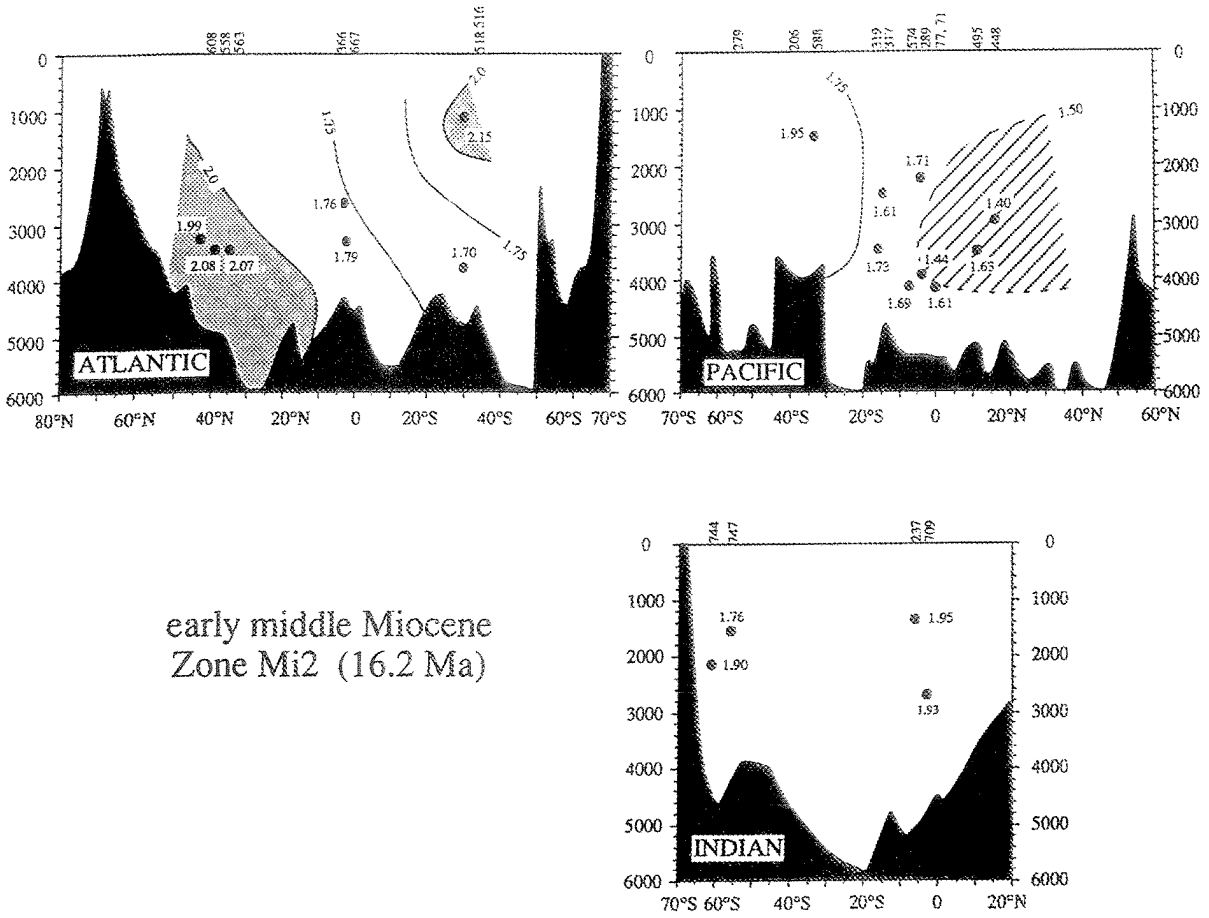

Fig. 13. Early/middle Miocene (Zone Mi2 - 16.2 Ma) boundary time slice reconstruction shows a north to south $\delta^{13}C$ gradient in the Atlantic Ocean. The North Atlantic recorded the highest $\delta^{13}C$ values, with the lowest $\delta^{13}C$ water mass in the intermediate North Pacific. A high $\delta^{13}C$ water mass apparently originated in the Southern Ocean and spread to the north at intermediate depths. High $\delta^{13}C$ values at Site 237 in the Indian Ocean are attributed to WSDW. Data for this reconstruction are in Table 2c.

hemisphere recorded high $\delta^{13}C$ values, indicating either the production of Tethyan water or SCIW with a high $\delta^{13}C$ value. As mentioned above, this signal was most prominent in the South Atlantic (Figure 13).

Middle Miocene Time Series

There are no deep Southern Ocean isotope records with adequate resolution for the middle Miocene time series reconstructions, limiting our interpretation of deepwater history for this interval. We can use the basin-basin $\delta^{13}C$ differences between the deep North Atlantic and Pacific for the middle Miocene time series. Miller and Fairbanks [1985] demonstrated that Atlantic-Pacific $\delta^{13}C$ differences provide a first-order proxy for NCW fluctuations. Carbon-isotope values in the North Atlantic and Pacific converged in the early middle Miocene (15.5 Ma) (Figure 14). This convergence signaled the shutdown of NCW production. As in the earliest Miocene, only SCW filled the Atlantic basins during the early middle Miocene, resulting in similar Atlantic and Pacific $\delta^{13}C$ values. Basin-basin $\delta^{13}C$ differences developed between 13 and 12 Ma, indicating that NCW production resumed (Figure 14). The magnitude of this difference reached only 0.5 ‰, one half of the modern difference. Lower Atlantic-Pacific $\delta^{13}C$ differences in the middle Miocene may partially reflect lower oceanic nutrient levels [Delaney, 1990; Wright et al., 1991] rather than lower fluxes of NCW. However, without a high-resolution Southern Ocean record, it is difficult to distinguish between lower NCW production or lower mean nutrient levels as the cause of these low interbasinal differences in $\delta^{13}C$ values.

Middle Miocene Time Slices

The early middle Miocene (Zone Mi3 - 13.6 Ma). A cross-sectional view of the early middle Miocene shows relatively uniform $\delta^{13}C$ values in the Atlantic Ocean (Figure 15). A small south to north gradient may have been present, but the difference between the Southern Ocean and the northern North Atlantic was only 0.2 ‰ (Figure 15). This south to north gradient reflects a weak or absent NCW flux. The cross-sectional view of the Pacific Ocean shows a larger south to

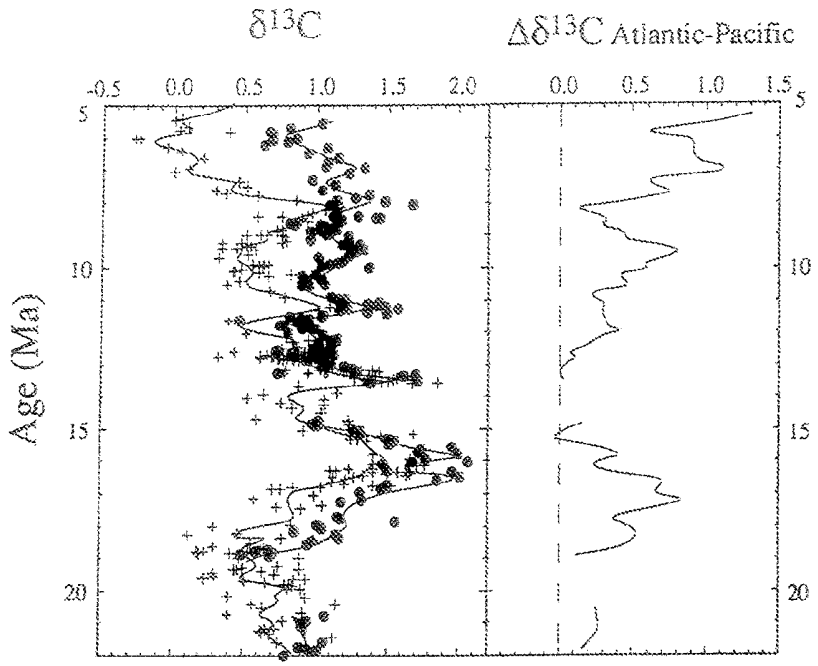

Fig. 14. Basin-basin $\delta^{13}C$ differences between the deep North Atlantic and the Pacific. These differences are used to estimate times of NCW production. Note that the largest basin-basin differences occurred between 19 and 16 Ma and later than 12.5 Ma.

north $\delta^{13}C$ gradient (0.7‰) than was recorded in the Atlantic. Deepwater aging is is the dominant process in the Pacific because its larger size and longer residence time of deep water. Indian Ocean $\delta^{13}C$ data show little latitudinal variation (Figure 15). The $\delta^{13}C$ data indicate that the SCW was the only source of deep water ventilating the oceans during the early middle Miocene.

The latest middle Miocene (Zone Mi5 - 11.3 Ma). The cross sectional view of the ocean in the latest middle Miocene (11.3 Ma) shows a different mode of deepwater circulation, as predicted by the Atlantic-Pacific $\delta^{13}C$ differences (Figure 16). As in the latest early Miocene, two high $\delta^{13}C$ water masses were produced in the late middle Miocene, NCW and SCIW. The deepwater $\delta^{13}C$ gradient within the Atlantic Ocean was from north to south (Figure 16), reversed from the south to north gradient earlier in the middle Miocene (Figure 15). The lowest $\delta^{13}C$ values in the deep ocean were found in the northern Indian and Pacific oceans (Figure 16). The $\delta^{13}C$ values in the intermediate northern Indian Ocean were low (Figure 16). This indicates that there was no WSDW source in the Tethys at this time, and that SCIW was the source of high $\delta^{13}C$ in the intermediate waters. SCIW displayed high $\delta^{13}C$ values, presumably in response to air-sea exchange processes [Charles and Fairbanks, 1990].

DISCUSSION

The $\delta^{13}C$ patterns presented above depict two modes of Miocene deepwater circulation. Southern Component Water was the only source of deep water during the earliest Miocene (24-20 Ma) and the early middle Miocene (15-12.5 Ma) (Figures 9, 11, and 15). A second mode occurred when SCW was supplemented by warmer, saltier water masses, NCW and Tethyan water during the late early Miocene (20-16 Ma), and NCW during the late middle Miocene (12.5-10 Ma) (Figures 9, 10, 12, 13, and 16) .

Sedimentation Patterns in the Early and Middle Miocene

Large-scale changes in deepwater circulation (i.e., the middle Miocene shutdown of NCW) should effect changes in sedimentation patterns. Several studies have documented the development of drift deposits in the North Atlantic during the early Miocene (see Shore and Poore [1979], Miller and Tucholke [1983] and DSDP Leg 94 for summaries). Large-scale drift deposition followed the erosion of Reflector R2, indicating an erosional pulse of deepwater followed by current controlled deposition [Miller and Tucholke, 1983]. The distribution of biogenic components (carbonate versus siliceous) can be affected as well by changing deepwater circulation patterns [Berger, 1970]. Three factors control the distribution of siliceous and carbonate sediments in the open ocean: (1) surface water productivity; (2) deepwater preservation; and (3) terrigenous dilution. In the absence of terrigenous dilution, Berger [1970] proposed that basin-basin fractionation between carbonate and siliceous sediments can develop in response to deepwater circulation patterns. Berger's model predicts that carbonate sedimentation would dominate in a basin with a lagoonal type circulation (surface inflow with outflow at depth; i.e., the modern Atlantic). In an estuarine basin (inflow at depth and surface outflow; i.e., the modern Pacific), siliceous sedimentation should be favored. This is an

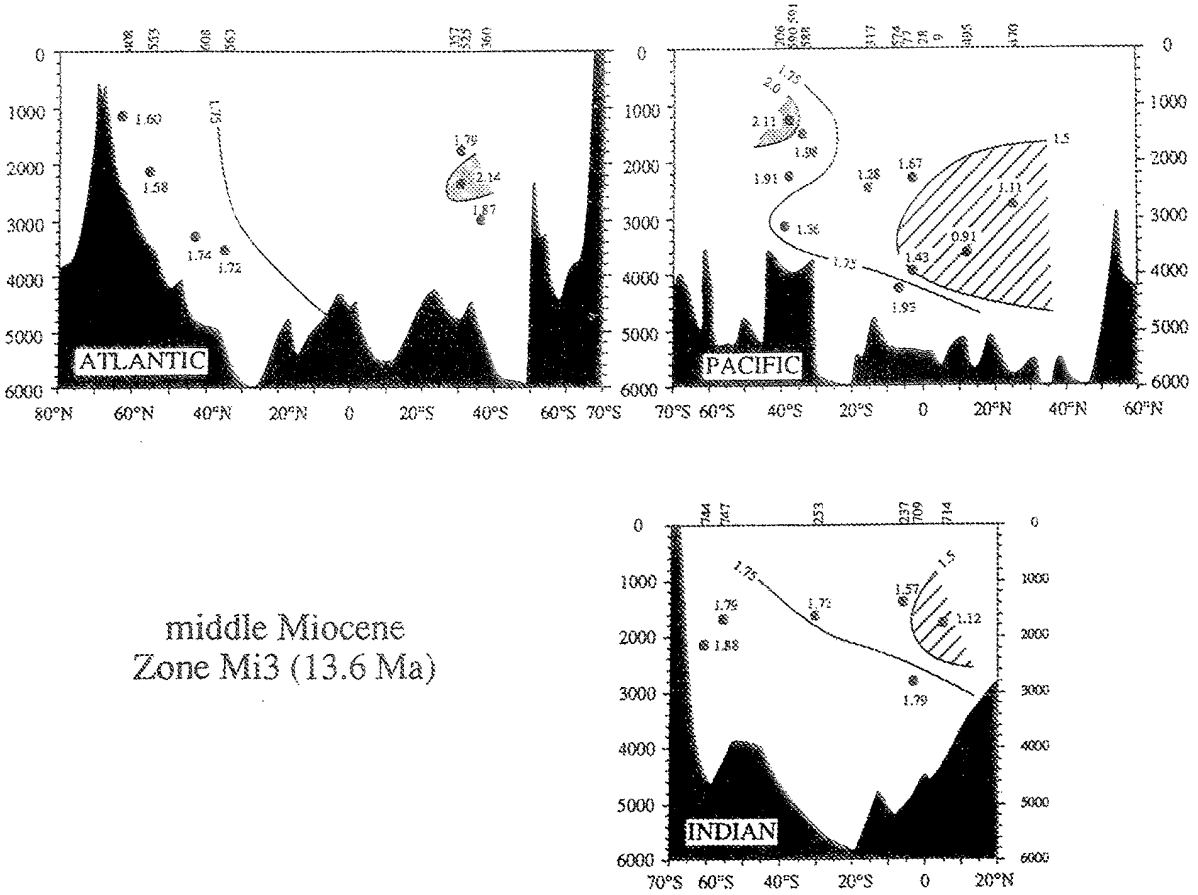

Fig. 15. Early middle Miocene (13.6 Ma) $\delta^{13}C$ reconstruction showing reduced $\delta^{13}C$ differences among all oceans. The Southern Ocean recorded the highest $\delta^{13}C$ values, with a low $\delta^{13}C$ water mass in the intermediate North Pacific. Data for this reconstruction are in Table 2d.

oversimplification of the system; however, we might expect to see some relationship between the general sedimentation patterns within the Atlantic and Pacific basins and the Miocene deepwater circulation patterns outlined above.

Keller and Barron [1983] attempted to relate biogenic sedimentation to deepwater circulation patterns. They portrayed the sedimentation patterns as a "silica switch" from the Atlantic to the Pacific around 15 Ma. This idea of a "silica switch" has propagated through the literature as evidence for NCW initiation in middle Miocene [e.g., Woodruff and Savin, 1989; Barron and Bauldauf, 1990; Maier-Reimer et al., 1990]. This general picture supports many of the deepwater circulation scenarios concerning the middle and late Miocene. In all scenarios, including Schnitker's [1980], Miller and Fairbanks' [1985], Woodruff and Savin's [1989], and this study's, one would expect basin-to-basin fractionation in carbonate and silica deposition to develop between the Atlantic and Pacific oceans during the late middle and late Miocene according to Berger's [1970] model.

A potential problem with the "silica switch" lies in the fact that Keller and Barron [1983] did not separate the biosiliceous components that are susceptible to dissolution (diatoms and silicoflagellates) from those that are resistant to dissolution (radiolarians and sponge spicules). Diatoms make up the bulk of siliceous productivity (95 to 98%), but are often not well preserved in the sediments. The presence of diatoms outside of upwelling regions is indicative of better silica preservation. The abundance of radiolarians and sponge spicules may or may not be diagnostic of preservation. These species are very resistant to dissolution and therefore are not necessarily indicative of silica preservation [Hurd and Theyer, 1975, 1977].

A reexamination of the original cores used by Keller and Barron [1983] shows that the early Miocene North Atlantic was not a siliceous basin (Figure 17). Previous inferences that biosiliceous accumulation in the North Atlantic was much higher during the early Miocene than during the middle and late Miocene are unsubstantiated. The Atlantic sites used in the original Keller and Barron [1983] study are best characterized as calcareous nannofossil and foraminiferal oozes with some intervals of clay accumulation (Figure 17). The biosiliceous component in most of these sites was minimal with sponge spicules and radiolaria as the primarily constituents.

Diatom preservation in the northern North Atlantic may

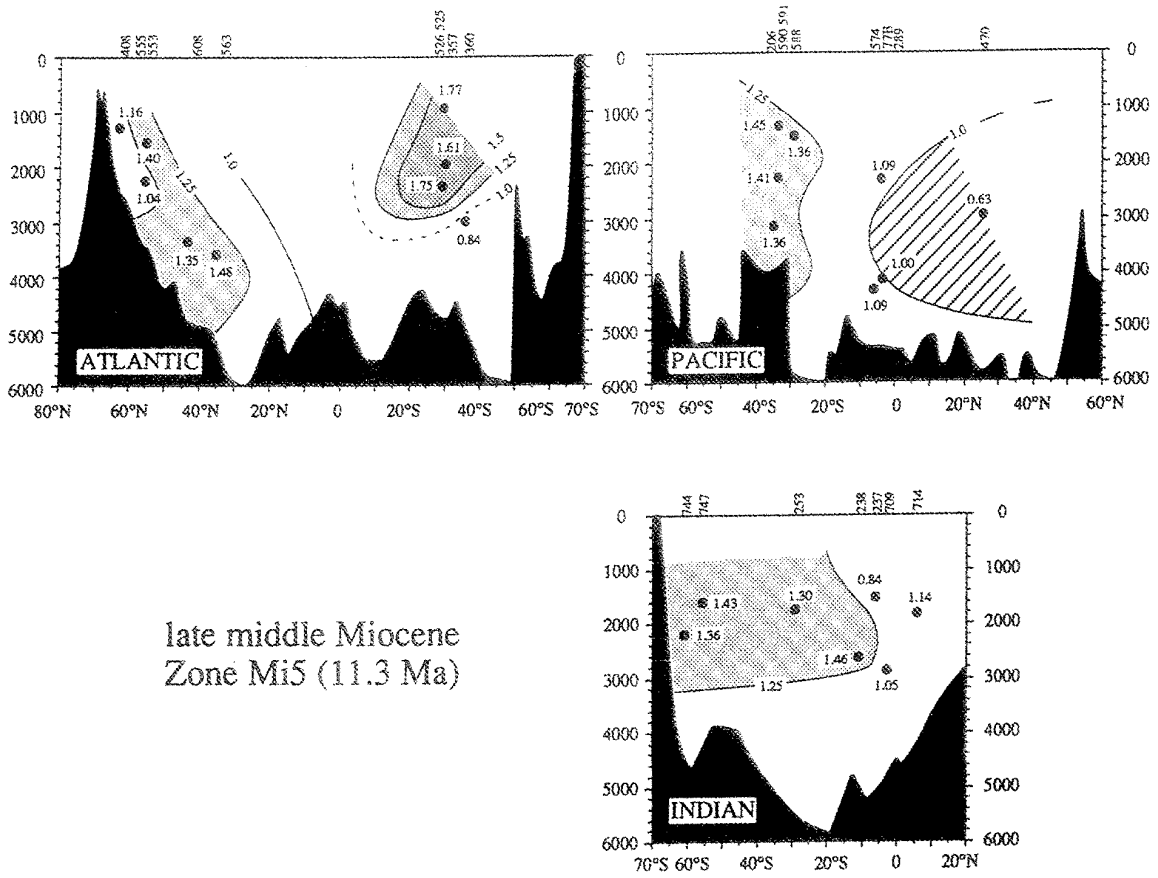

Fig. 16. Late middle Miocene (11.3 Ma) $\delta^{13}C$ reconstruction which again recorded a north to south $\delta^{13}C$ gradient in the Atlantic Ocean. The North Atlantic recorded the highest $\delta^{13}C$ values, with the lowest $\delta^{13}C$ values in the intermediate North Pacific. A high $\delta^{13}C$ water mass apparently originated in the Southern Ocean and spread to the north at intermediate depths. Low $\delta^{13}C$ values at Indian Ocean Site 714 indicate that no WSDW originated in the Indian Ocean. Data for this reconstruction are in Table 2e.

provide the most appropriate assessment of the relationship between silica preservation and NCW production during the early Miocene. Bauldauf [1987] assessed diatom preservation at Sites 406 and 610, both located in the northeastern Atlantic near the Rockall Plateau (Figure 2). On the basis of an integrated magnetobiostratigraphic age model, intervals of good to moderate preservation at Site 610 occurred from 21 to 19 Ma and 16 to 13 Ma, while poor preservation occurred from 19 to 16 Ma (Figure 17). Diatom assemblages at Site 406 recorded a similar cycle (Figure 17). Earliest Miocene (~24 to 23 Ma) diatom preservation was good at this site [Bauldauf, 1987]. A hiatus separates the earliest Miocene from the latest early Miocene, when diatom assemblages were poorly preserved (~17 to 16 Ma). This brief interval was followed by a second interval of good preservation from ~16 to 15 Ma (Figure 17).

The preservation of diatoms in the northeast Atlantic is consistent with our deepwater circulation patterns identified using $\delta^{13}C$ distributions. In the earliest Miocene (24 to 20 Ma), diatoms assemblages were well preserved during the interval of little to no NCW production (Figures 9 and 10). Diatom preservation changed from moderate to poor at 19 Ma at Site 610 and remained poor into the middle Miocene [Bauldauf, 1987]. This interval of poor preservation coincided with an interval of vigorous NCW production. Diatom preservation improved from poor to moderate at Sites 406 and 610 above the early/middle Miocene boundary (~16 Ma) [Bauldauf, 1987]. Again, the change in diatom preservation coincided with the shutdown of NCW production. This assessment of diatom preservation should be verified in other parts of the North Atlantic.

Climate Changes and Deepwater Circulation in the Early and Middle Miocene

Our scenario invokes poleward heat transport to warm the deep oceans during the early and middle Miocene through the production of relatively warm, deep water masses (NCW and/or Tethyan outflow water). This idea is similar to previous hypotheses [e.g., Shackleton and Kennett, 1975; Savin et al., 1975; Kennett, 1985; Prentice and Matthews, 1988; Woodruff

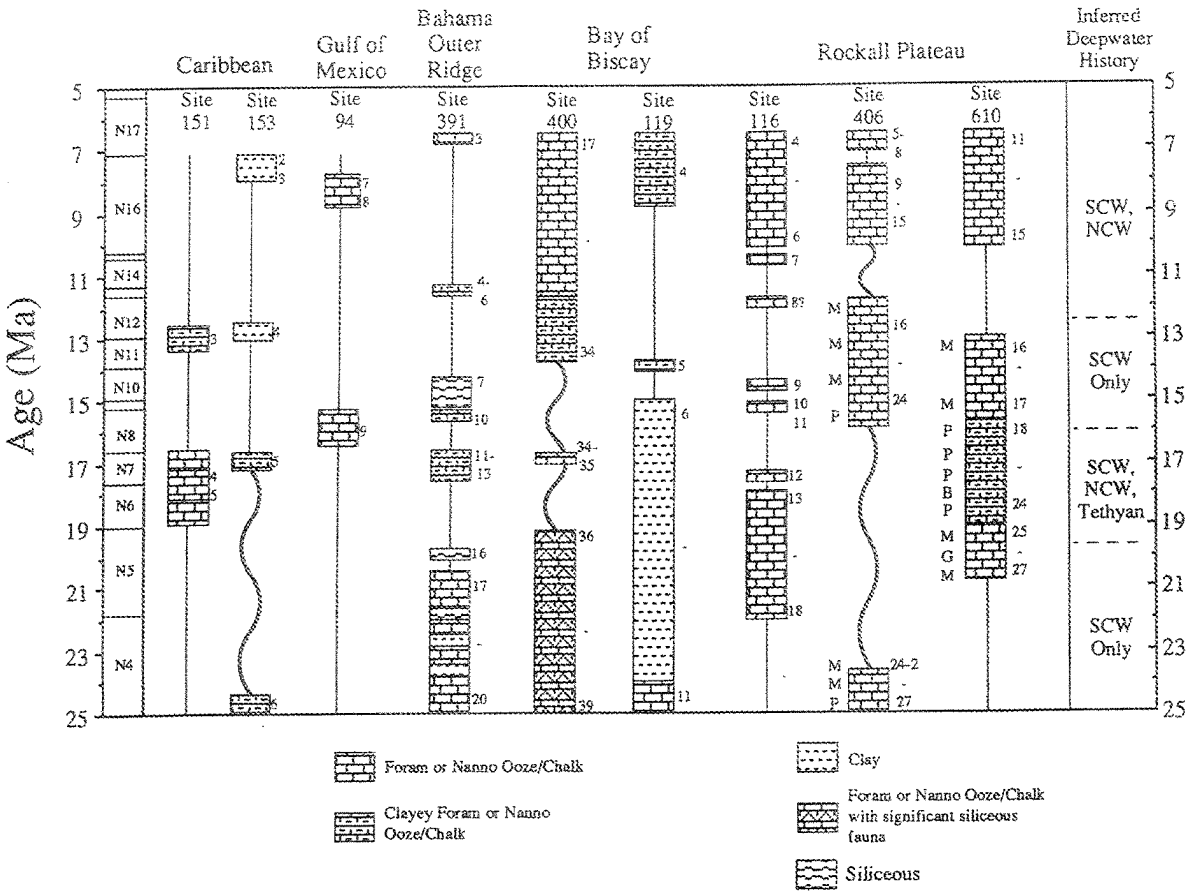

Fig. 17. Distribution and type of sediments within the North Atlantic during the Miocene. Site selection was similar to the Keller and Barron [1983] study. Age and sediment type was taken from site chapter reports for each site. Core numbers are placed to the right of each section. Diatom preservation for Sites 406 and 610 is denoted by "P", "M", and "G" for poor, moderate, and good, respectively, and is found to the left of these sites [after Bauldauf, 1987]. Our interpretation of Miocene deepwater circulation changes is provided in the far right column.

and Savin, 1989], and it is consistent with consequences associated with late Pleistocene climate changes. For example, NADW is 1.5 to 2°C warmer than AABW at present; it is considered an important source of heat and salt to the deep ocean and high southern latitudes [Worthington, 1970; Gordon and Piola, 1983; Jacobs et al., 1985]. Deepwater temperatures were cooler by ~1.5°C during the last glacial when NADW production was reduced [Chappell and Shackleton, 1986]. We investigate below the relationship between early to middle Miocene deepwater circulation changes and climate changes recorded in benthic foraminiferal $\delta^{18}O$ records.

A general interpretation of Miocene benthic foraminiferal $\delta^{18}O$ records indicates that deepwaters warmed from the earliest Miocene (~24 Ma), recording maximum temperatures near the early/middle Miocene boundary (17 and 15 Ma) (Figure 18) [Shackleton and Kennett, 1975; Savin et al., 1975, 1981; Prentice and Matthews, 1988]. Benthic foraminiferal $\delta^{18}O$ values increased between 15 and 12 Ma as the result of Antarctic ice growth and a decrease in deepwater temperatures [Shackleton and Kennett, 1975; Savin et al., 1975]. This long-term trend of deepwater warming and subsequent cooling coincided with early Miocene production of NCW and Tethyan outflow water and the subsequent reduction of both around 15 Ma. However, the relative contributions from temperature and ice volume during the middle Miocene $\delta^{18}O$ increase can only be resolved by considering planktonic foraminiferal $\delta^{18}O$ records from western equatorial locations [Shackleton and Opdyke, 1973].

Ice Volume Changes in the Miocene

Low-latitude planktonic-benthic foraminiferal $\delta^{18}O$ covariance provides the best estimate of ice volume changes [Shackleton and Opdyke, 1973]. Miller et al. [1991a, also manuscript in preparation, 1992] compared the planktonic foraminiferal $\delta^{18}O$ record from Sites 237 and 707 (western equatorial Indian Ocean) and a benthic foraminiferal $\delta^{18}O$ record from Site 563 for the middle Miocene $\delta^{18}O$ increase. Covariance between these records shows $\delta^{18}O$ amplitudes of 0.5 to a 0.8 ‰ for this interval. In a similar fashion, we note that low-latitude planktonic foraminiferal $\delta^{18}O$ values from

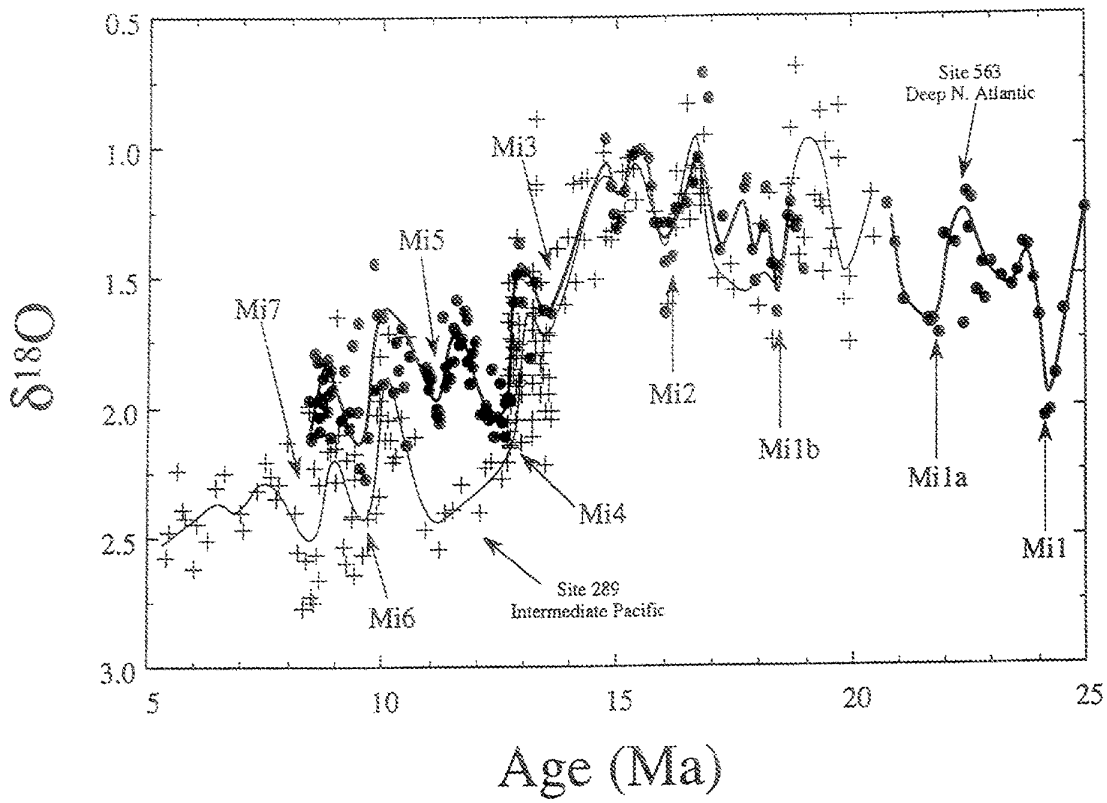

Fig. 18. Benthic $\delta^{18}O$ records from Sites 563 and 289. "Mi" events are identified on each curve [Miller et al., 1991a; Wright and Miller, 1992a]. The long-term trend in the Miocene was a decrease in $\delta^{18}O$ values from the earliest Miocene to the early middle Miocene and an increase in $\delta^{18}O$ values beginning around 15 Ma.

other sites recorded 0.8 ‰ increase on average during the middle Miocene $\delta^{18}O$ increase (Zones Mi3 and Mi4; 15 to 12.5 Ma) (Sites 214, 216, 237, 289, 366, and 707) (Figure 19). The average benthic foraminiferal $\delta^{18}O$ increase over the same interval was 1.3 ‰. The excess global $\delta^{18}O$ change in the benthic foraminifera (0.5 ‰) must reflect deepwater cooling. A similar temperature change might be expected for high-latitude surface waters. Planktonic foraminiferal $\delta^{18}O$ records from the middle and high latitudes recorded $\delta^{18}O$ increases that were greater than those in the equatorial regions. Subtropical surface waters recorded an increase of ~1.0 ‰ (Sites 563 and 590), while the high latitudes recorded a 1.3 ‰ increase (Site 751) (Figure 19). This increase in the meridional surface water $\delta^{18}O$ gradient reflects a high-latitude cooling of 2.5°C, which was recorded in deep waters as well.

The planktonic-benthic foraminiferal $\delta^{18}O$ covariance associated with other "Mi" events ranged from 0.5 to 0.8 ‰ (Table 4). This suggests that Antarctic ice sheets waxed and waned throughout the early and middle Miocene, resulting in million year scale glacial-interglacial cycles. The magnitude of these ice volume changes can be compared to the modern Antarctic ice sheet. Shackleton and Kennett [1975] estimated that the $\delta^{18}O_{water}$ change associated with the melting of the present Antarctic ice sheet to be ~0.9 ‰. Therefore estimated Miocene ice volume induced $\delta^{18}O$ changes ranged from 60 to 90 % of the modern Antarctic ice sheet.

The ice volume/$\delta^{18}O_{water}$ changes can be translated into sea level equivalents by applying a $\delta^{18}O_{water}$/sea level calibration. Fairbanks and Matthews [1978] measured this to be 0.11 ‰/10 m sea level change for the late Pleistocene oceans. The calibration may have been different under conditions warmer than the Pleistocene. Miller et al. [1987] noted that the extreme limit for the pre-Pleistocene sea level calibration is 0.055 ‰/10 m sea level change for the older oceans. Therefore sea level changes of 50 to 80 m (modern calibration) are suggested by the planktonic-benthic foraminiferal $\delta^{18}O$ covariance. These sea level changes should be recorded by sedimentary sequences on passive continental margins. Miller et al. [1991a, also manuscript in preparation, 1992] have documented a good coherence between the "Mi" increases and the Type 1 sequence boundaries identified by Haq et al. [1987]. This provides independent evidence that the "Mi" zones represent separate ice volume events.

Deepwater Temperature Reconstruction

Deepwater temperature changes can be estimated for the early to middle Miocene because the timing is well constrained and magnitudes of ice volume/$\delta^{18}O_{water}$ changes can be

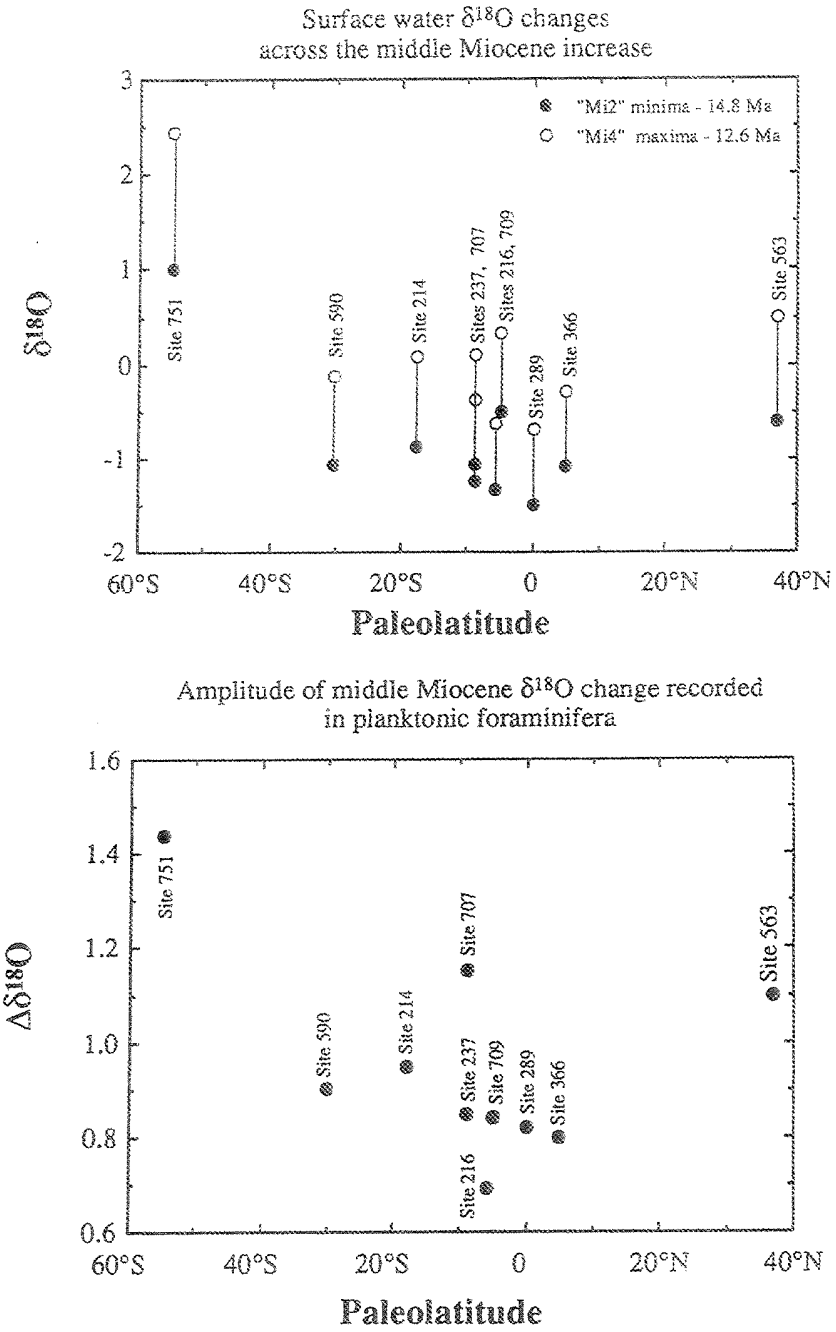

Fig. 19. (a) Planktonic foraminiferal $\delta^{18}O$ values prior to the middle Miocene $\delta^{18}O$ increase ("Mi2 interglacial," solid circles) and at the base of the increase (Mi4, open circles). (b) $\delta^{18}O$ difference recorded during the middle Miocene increase. The largest $\delta^{18}O$ increase was recorded in the high latitudes.

estimated. The deepwater temperature estimates presented below represent long-term changes. We are cognizant of higher-frequency changes (orbital) that were superimposed on the million year records [Pisias et al., 1985]. However, we are concerned with portraying the deepwater temperature history with a resolution similar to that in our carbon isotope-based deepwater circulation reconstructions, which is of the order of one million years.

As noted previously, early Miocene benthic foraminiferal $\delta^{18}O$ values increased from a maximum at the Oligocene/Miocene boundary to a minimum around the early/middle Miocene boundary (Figure 18). Miller et al. [1991a] and

TABLE 4. Oxygen Isotope Increase Associated With Each "Mi" Event

Event	Age Ma	Benthic	Planktonic	Covariance	Sites
Mi1	23.7	0.8 ‰	0.8 ‰	0.8 ‰	Benthic - Sites 563, 608, 747 Planktonic - Site 558
Mi1a	21.7	0.5 ‰			Benthic - Sites 563, 608, 747
Mi1aa	20.0	0.5 ‰			Benthic - Sites, 289, 747
Mi1b	18.3	0.5 ‰	0.7 ‰	0.5 ‰	Benthic - Sites 563, 608, 747 Planktonic - Site 707
Mi2	16.2	0.8 ‰	0.7 ‰	0.7 ‰	Benthic - Sites 563, 608, 747 Planktonic - Sites 237, 289, 366, 707
Mi3	13.6	0.8 ‰	0.75 ‰	0.75 ‰	Benthic - Sites 563, 608, 747 Planktonic - 237, 289, 707
Mi4	12.6	0.8 ‰	0.7 ‰	0.7 ‰	Benthic - Sites 563, 608, 747 Planktonic - Sites 237, 289
Mi5	11.3	0.6 ‰	0.6 ‰	0.6 ‰	Benthic - Sites 563, 608, 747 Planktonic - Sites 289, 707

Wright and Miller [1992a] identified four glacial/interglacial cycles which were superimposed on this long-term trend (Mi1, Mi1a, Mi1b, Mi2). We note that an additional $\delta^{18}O$ maximum (equal to inferred glacial maximum) occurred at approximately 20 Ma [Wright and Miller, 1992a]. Because $\delta^{18}O_{water}$ values varied with ice volume changes during the early Miocene, relative deepwater temperature changes must be estimated for times when the ice volumes/$\delta^{18}O_{water}$ were similar. We speculate that the ice volumes were similar for each of the glacial/$\delta^{18}O$ maxima as well as for each of the $\delta^{18}O$ minima. This assumption allows us to evaluate the temperature component of the benthic foraminiferal changes between the $\delta^{18}O$ maxima and minima. Therefore the differences in absolute values ($\Delta\delta^{18}O$) among the "Mi" $\delta^{18}O$ maxima, as well as the $\delta^{18}O$ minima, reflect deepwater temperature changes.

In the early Miocene, the $\delta^{18}O$ values for the "Mi1", "Mi1a", "Mi1b", and Mi2" maxima were 2.1, 1.75, 1.5, and 1.4 ‰, respectively (Figure 18). If these were times of roughly equivalent ice volumes/$\delta^{18}O_{water}$, then the deepwater $\delta^{18}O$ change of 0.7 ‰ corresponds to a ~3°C warming (Figures 18, 20). Similarly, the $\delta^{18}O$ minima recorded a decrease from 1.4 to 0.8 ‰ between 23 and 17 Ma (Figures 18 and 20), which corresponds to a 2.5°C warming (Figures 18, 20). Thus temperature estimates derived from comparison of the $\delta^{18}O$ maxima and minima yield similar deepwater temperature changes.

If we apply this method to the middle Miocene (Figure 20), we see that: (1) a minor deepwater cooling of 1° to 2°C occurred from 17 to 15 Ma prior to the middle Miocene $\delta^{18}O$ increase; (2) further deepwater cooling of 2.5°C occurred during the $\delta^{18}O$ shift; and (3) North Atlantic temperatures remained constant from 12.5 to 10 Ma while Pacific deep waters continued to cool by as much as 2°C. We note that this method and the planktonic-benthic foraminiferal covariance method yield the same results concerning the middle Miocene $\delta^{18}O$ increase: an ice volume effect of 0.8 ‰ with a temperature decrease of 2° to 2.5°C.

CONCLUSIONS

Carbon isotope patterns indicate that two modes of deepwater circulation operated during the early and middle Miocene. The deep oceans were ventilated by only SCW during the intervals from 24 to 20 Ma and 16 to 12.5 Ma. In contrast, multiple deepwater sources operated during the other intervals of the early to middle Miocene. Relatively warm NCW and Tethyan water masses supplemented SCW production from 20 to 16 Ma, while NCW and SCW were produced from 12.5 to 10 Ma.

The combination of NCW and Tethyan water masses from 20 to 16 Ma produced a significant meridional heat flux that warmed the deep ocean by 3 to 4 °C. Deepwater temperatures cooled after the fluxes of NCW and Tethyan water were reduced around 16 Ma. The deep oceans have remained relatively cold since. However, renewed production of NCW during the late middle and late Miocene appears to have warmed the North Atlantic by ~2°C relative to the Pacific and Southern oceans.

Miocene intermediate waters were ventilated by Southern Component Intermediate Water (SCIW) originating in the Southern Ocean. This water mass was present in the southern hemisphere of Atlantic, Pacific, and Indian oceans. SCIW recorded high $\delta^{13}C$ values during the Miocene as a result of isotopic fractionation in the SCIW source regions of CO_2 through either air-sea exchange processes and/or a biological stripping of nutrients.

The middle Miocene $\delta^{18}O$ increase resulted from a combination of increasing ice volume and deepwater cooling. Our data suggest that this $\delta^{18}O$ increase was part of two to three glacial-interglacial cycles during the middle Miocene [Miller et al., 1991a; Wright and Miller, 1992a] and not the transition from an ice-free to an ice house world. These

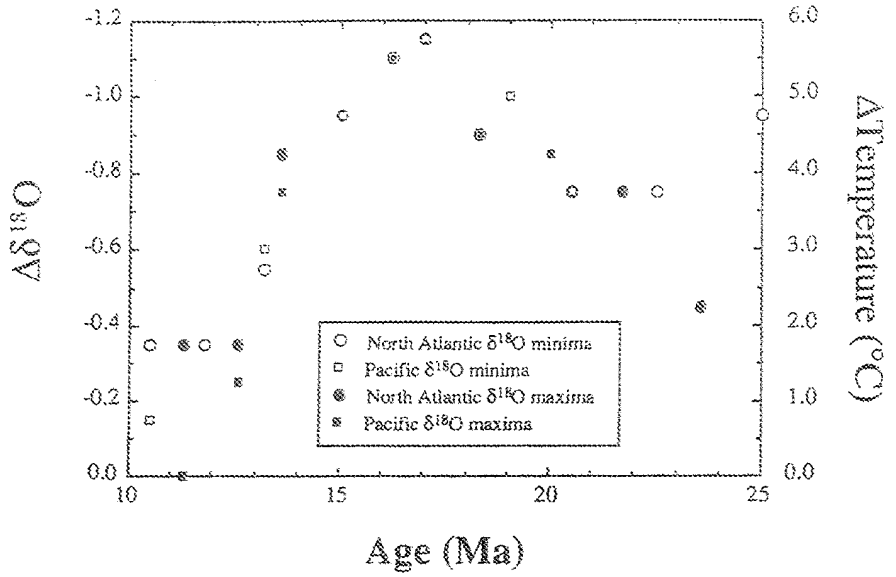

Fig. 20. Relative $\delta^{18}O$ differences ($\Delta\delta^{18}O$) between the "Mi interglacials" (open symbols) and "Mi" events (solid symbols) for the North Atlantic (circles) and Pacific (boxes) Oceans during the early and middle Miocene. Pacific Site 289 was selected as the reference point to determine $\Delta\delta^{18}O$ values for the early to middle Miocene "Mi" events because this site is the best representative of mean deepwater conditions. The "Mi5" glacial and interglacial datums (2.45 and 1.95 ‰, respectively) were set arbitrarily as zero. Relative temperature changes were obtained by assuming that ice volumes were similar for each "Mi interglacial" and for each "Mi" event.

million year glacial-interglacial cycles do not correlate to deepwater circulation changes, in contrast to deepwater temperatures that show a good correspondence to deepwater circulation changes.

Acknowledgments. We thank J. Zachos and F. Woodruff for critical reviews which improved this manuscript greatly. M. E. Katz provided technical assistance through out the project. W. F. Ruddiman, R. Z. Poore, and D. V. Kent provided helpful comments on an early version of this manuscript. This work was supported by NSF Grants OCE85-21690 and OCE88-11834 to K. Miller and OCE88-19438 and OCE91-17111 to R. Fairbanks. This is Lamont-Doherty Geological Observatory contribution 4938.

REFERENCES

Barker, P. F., and J. Burrell, The opening of Drake Passage, *Mar. Geol., 25*, 15-34, 1977.

Barker, P. F., et al., *Proc. Ocean Drill. Prog., Initial Repts.*, vol. 113, 1033pp., Ocean Drilling Program, College Station, Tex., 1988.

Barrera, E., and B. T. Huber, Paleogene and early Neogene oceanography of the southern Indian Ocean: Leg 119 foraminifer stable isotope results, *Ocean Drill. Program, Sci. Results, 119*, 693-717, 1991.

Barrera, E., G. Keller, and S. M. Savin, Evolution of the Micene ocean in the eastern North Pacific as inferred from oxygen and carbon isotopic ratios of foraminifera, in The Miocene Ocean: Paleoceanography and Biogeography, edited by J. P. Kennett, *Mem. Geol. Soc. Am., 163*, 83-102, 1985.

Barrera, E., B. T. Huber, S. M. Savin, and P.-N. Webb, Antarctic marine temperatures: Late Campanian through early Paleocene, *Paleoceanography, 2*, 21-47, 1987.

Barrett, P. J., D. P. Elston, D. M. Harwood, B. C. McKelvey, and P.-N. Webb, Mid-Cenozoic record of glaciation and sea level change on the margin of the Victoria Land Basin, Antarctica, *Geology, 15*, 634-637, 1987.

Barron, J .A., et al., *Proc. Ocean Drill. Prog., Initial Repts.*, vol. 119, 939pp., Ocean Drilling Program, College Station, Tex., 1989.

Barron, J. A., and J. G. Bauldauf, Development of biosiliceous sedimentation in the North Pacific during the Miocene and early Pliocene, in *Pacific Neogene Events*, edited by R. Tsuchi, pp. 43-63, University of Tokyo Press, Tokyo, 1990.

Barron, E. J., S. L. Thompson, and S. H. Schneider, An ice-free Cretaceous? Results from climate model simulations, *Science, 212*, 501-508, 1981.

Bauldauf, J. G., Biostratigraphic and paleoceanographic interpretation of lower and middle Miocene sediments, Rockall Plateau region, North Atlantic Ocean, *Initial Rep. Deep Sea Drill. Proj., 94*, 1033-1043, 1987.

Belanger, P. E., W. B. Curry, and R. K. Matthews, Core-top evaluation of benthic foraminiferal isotopic ratios for paleo-oceanographic interpretations, *Paleogeogr. Palaeoclimatol. Palaeoecol., 33*, 205-220, 1981.

Berger, W. H., Biogenous deep-sea sediments: Fractionation by deep-sea circulation, *Geol. Soc. Am. Bull., 81*, 1385-1402, 1970.

Berggren, W. A., and C. D. Hollister, Plate tectonics and paleocirculation - Commotion in the ocean, *Tectonophysics, 38*, 11-48, 1977.

Berggren, W. A., D. V. Kent, and J. A. Van Couvering, Neogene geochronology and chronostratigraphy, The Chronology of the Geological Record, edited by N. J. Snelling, *Mem. Geol. Soc. London, 10*, 211-260, 1985.

Blanc, P.-L., and J. C. Duplessy, The deep-water circulation during the Neogene and the impact of the Messinian salinity crisis, *Deep Sea Res., 29 Part A*, 1391-1414, 1982.

Blanc, P.-L, D. Rabussier, C. Vergnaud-Grazzini, and J.-C. Duplessy, North Atlantic Deep Water formed by the later middle Miocene, *Nature, 283*, 553-555, 1980.

Boersma, A., and N. Mikkelsen, Miocene-age primary productivity episodes and oxygen minima in the central equatorial Indian Ocean, *Proc. Ocean Drill. Program, Sci. Results, 115*, 589-610, 1990.

Boyle, E. A., The role of vertical chemical fractionation in controlling late Quaternary atmospheric carbon dioxide, *J. Geophys. Res., 93*, 15,701-15,714, 1988.

Boyle, E. A., and L. D. Keigwin, Deep circulation of the North Atlantic over the last 200,000 years, geochemical evidence, *Science, 218*, 784-787, 1982.

Boyle, E. A., and L. D. Keigwin, North Atlantic thermohaline circulation during the past 20,000 years linked to high-latitude surface temperature, *Nature, 330*, 35-40, 1987.

Broecker, W. S., and T.-H. Peng, *Tracers in the Sea*, 690 pp., Eldigio, Palisades, N. Y., 1982.

Broecker, W. S., M. Andree, W. Wolfli, H. Oeschger, G. Bonani, J. Kennett, and D. Peteet, The chronology of the Last Deglaciation: Implications to the cause of the Younger Dryas Event, *Paleoceanography, 3*, 1-19, 1988.

Broecker, W. S., T.-H. Peng, S. Trumbore, G. Bonani, and W. Wolfli, The distribution of radiocarbon in the glacial ocean, *Global Biogeochem. Cycles, 4*, 103-117, 1990.

Chappell, J., and N. J. Shackleton, Oxygen isotopes and sea level, *Nature, 324*, 137-140, 1986.

Charles, C.D., Late Quaternary ocean chemistry and climate change from an Antarctic deep sea sediment perspective, Ph.D thesis, 181 pp., Columbia Univ., N. Y., 1991.

Charles, C. D., and R. G. Fairbanks, Glacial to intergiacial changes in the isotopic gradients of Southern Ocean surface water, in *Geologic History of the Polar Oceans: Arctic Versus Antarctic*, edited by U. Bleil and J. Thiede, pp. 519-538, Kluwer Academic, Boston, Mass., 1990.

Charles, C. D., and R. G. Fairbanks, Evidence from Southern Ocean sediments for the effect of North Atlantic deep-water flux on climate, *Nature, 355*, 416-419, 1992.

Ciesielski, P. F., et al., *Proc. Ocean Drill. Prog., Initial Repts.*, vol. 114, 811pp., Ocean Drilling Program, College Station, Tex., 1988.

Curry, W. B. and G .P. Lohmann, Carbon isotopic changes in benthic foraminifera from the western South Atlantic: Reconstruction of glacial abyssal circulation patterns, *Quat. Res., 18*, 218-235, 1982.

Curry, W. B., J.-C. Duplessy, L. D. Labeyrie, and N. J. Shackleton, Quaternary Deep-water circulation changes in the distribution of $\delta^{13}C$ of deep water ΣCO_2 between the last glaciation and the Holocene, *Paleoceanography, 3*, 317-341, 1988.

Delaney M. L., Miocene benthic foraminiferal Cd/Ca records: South Atlantic and western equatorial Pacific, *Paleoceanography, 5*, 743-760, 1990.

Delaney M. L., and E. A. Boyle, Cd/Ca in late Miocene benthic foraminifera and changes in the global organic carbon budget, *Nature, 330*, 156-159, 1987.

Duplessy, J.-C., C. Lalou, and A. C. Vinot, Differential isotopic fractionation in benthic foraminifera and paleotemperatures reassessed, *Science, 168*, 250-251, 1970.

Duplessy, J.-C., N. J. Shackleton, R. G. Fairbanks, L. Labeyrie, D. Oppo, and N. Kallel, Deep-water source variations during the last climatic cycle and their impact on the global deepwater circulation, *Paleoceanography, 3*, 343-360, 1988.

Fairbanks, R. G. and R. K. Matthews, The marine oxygen isotope record in Pleistocene coral , Barbados, West Indies, *Quat. Res., 10*, 181-196, 1978.

Foster, T. D., and E. C. Carmack, Frontal zone mixing and Antarctic Bottom Water formation in the southern Weddell Sea, *Deep-Sea Res., 23*, 301-317, 1976.

Gordon, A. L., Seasonality of Southern Ocean sea ice, *J. Geophys. Res., 86*(C5), 4193-4197, 1981.

Gordon, A. L., and A. R. Piola, Atlantic Ocean upper layer salinity budget, *J. Phys. Oceanogr., 13*, 1293-1300, 1983.

Graham, D. W., B. H. Corliss, M. L. Bender, and L. D. Keigwin, Carbon and oxygen isotopic disequilibria of Recent benthic foraminifera, *Mar. Micropaleontol., 6*, 483-497, 1981.

Haq, B. U., J.Hardenbol, P. R. Vail, Chronology of fluctuating sea levels since the Triassic (250 million years to present), *Science, 235*, 1156-1167, 1987.

Hurd, D. C. and F. Theyer, Changes in the physical and chemical properties of biogenic silica from the central equatorial Pacific, in *Advances in Chemistry Series*, vol. 147, edited by R. P. Gibb, Jr., pp. 211-230, American Chemical Society, 1975.

Hurd, D. C. and F. Theyer, Changes in the physical and chemical properties of biogenic silica from the central equatorial Pacific: Part II. Refractive index, density, and water content of acid-cleaned samples, *Am. J. Sci., 277*, 1168-1202, 1977.

Jacobs, S. S., R. G. Fairbanks, and Y. Horibe, Origin and evolution of water masses near the Antarctic continental margin: Evidence from $H_2{}^{18}O/H_2{}^{16}O$ ratios in seawater , in Oceanology of the Antarctic Continental Shelf, *Antart. Res. Ser.*, vol. 43, edited by S. S. Jacobs, pp. 59-85, AGU, Washington, D. C., 1985.

Jones, E. J., M. Ewing, J. I. Ewing, and S. L. Eittreim, Influences of Norwegian Sea overflow water on sedimentation in the northern North Atlantic and Labrador Sea, *J. Geophys, Res., 75*, 1655-1680, 1970.

Keigwin, L. D., M.-P. Aubry, and D.V. Kent, North Atlantic late Miocene stable-isotope stratigraphy, biostratigraphy, and magnetostratigraphy, *Initial Rep. Deep Sea Drill. Proj., 94*, 935-963, 1986.

Keller, G., and J. A. Barron, Paleoceanographic implications of Miocene deep-sea hiatuses, *Geol. Soc. Am. Bull., 94*, 590-613, 1983.

Kennett, J. P., The Miocene Ocean: Paleoceanography and Biogeography, edited by J. P. Kennett, *Mem. Geol. Soc. Am., 163*, 337 pp., 1985.

Kennett, J. P., Miocene to early Pliocene oxygen and carbon isotope stratigraphy in the southwest Pacific, Deep Sea Drilling Project Leg 90, *Initial Rep. Deep Sea Drill. Proj., 90*, 1383-1411, 1986.

Kennett, J. P. and P. F. Barker, Latest Cretaceous to Cenozoic

climate and oceanographic developments in the Weddell Sea, Antarctica: An ocean-drilling perspective, in *Proc. Ocean Drill. Program Sci. Results, 113*, 937-960, 1990.

Kroopnick, P., The distribution of ^{13}C of ΣCO_2 in the world oceans, *Deep Sea Res., 32*, 57-84, 1985.

Lawver, L. A., L. M. Gahagan, and M. F. Coffin, Plate reconstructions and the development of seaways in the Circum-Antarctic region, Internat. Conference on the Role of Southern Ocean in Global Change: An Ocean Drilling Perspective, *Abstracts, 29*, 1991.

Mackensen, A., E. Barrera, and H.-W. Hubberten, Neogene circulation in the southern Indian Ocean: Evidence from benthic foraminifer assemblages, carbonate data, and stable isotope analyses (Site 751), in *Proc. Ocean Drill. Program Sci. Results*, 120, in press, 1992.

Maier-Reimer, E., U. Mikolajewicz, and T. J. Crowley, Ocean general circulation model sensitivity experiment with an open Central American Isthmus, *Paleoceanography, 5*, 349-366, 1990.

Mantyla, A. W., and J. L. Reid, Abyssal characteristics of the World Ocean waters, *Deep Sea Res., Part A, 8*, 805-833, 1983.

Matthews, R. K., and R. Z. Poore, Tertiary $\delta^{18}O$ record and glacio-eustatic sea-level fluctuations, *Geology, 8*, 501-504, 1980.

Miller, K. G., Middle Eocene to Oligocene stable isotopes, climate, and deepwater history: The Terminal Eocene Event? in *Eocene-Oligocene Climatic and Biotic Evolution*, edited by D. Prothero and W. W. Berggren, Princeton University Press, Princeton, NJ, in press, 1992.

Miller, K. G., and W. B. Curry, Eocene to Oligocene benthic foraminiferal isotopic record in the Bay of Biscay, *Nature, 296*, 347-350, 1982.

Miller, K. G. and R. G. Fairbanks, Oligocene to Miocene carbon isotope cycles and abyssal circulation changes, in *The Carbon Cycle and Atmospheric CO_2: Natural Variations Archean to Present. Geophys. Monogr. Ser.*, vol. 32, edited by E. T. Sunquist and W. S. Broecker, pp. 469-486, AGU, Washington, D. C., 1985.

Miller, K., and D. V. Kent, Testing Cenozoic eustatic changes: The critical role of stratigraphic resolution, *Cushman Foundation Foram. Res.Spec. Publ., 24*, 51-56, 1987.

Miller, K. G., and B. E. Tucholke, Development of Cenozoic abyssal circulation south of the Greenland-Scotland Ridge, in *Structure and Development of the Greenland-Scotland Ridge*, edited by M. H. P. Bott et al., pp. 549-589, Plenum, New York, 1983.

Miller, K. G., M.-P. Aubrey, M. J. Khan, A. J. Melillo, D. V. Kent, and W. A. Berggren, Oligocene-Miocene biostratigraphy, magnetostratigraphy and isotopic stratigraphy of the western North Atlantic, *Geology, 13*, 257-261, 1985.

Miller, K. G., R. G. Fairbanks, and E. Thomas, Benthic foraminiferal carbon isotopic records and the development of abyssal circulation in the eastern North Atlantic, *Initial Rep. Deep Sea Drill. Proj., 94*, 981-996, 1986.

Miller, K. G., R. G. Fairbanks, and G. S. Mountain, Tertiary oxygen isotope synthesis, sea level history, and continental margin erosion, *Paleoceanography, 2*, 1-19, 1987.

Miller, K. G., M. D. Feigenson, D. V. Kent, and R. K. Olsson, Oligocene stable isotope ($^{87}Sr/^{86}Sr$, $\delta^{18}O$, $\delta^{13}C$) standard section, Deep Sea Drilling Project Site 522, *Paleoceanography, 3*, 223-233, 1988.

Miller, K. G., J. D. Wright , A. N. Brower, Oligocene to Miocene stable isotope stratigraphy and planktonic foraminiferal biostratigraphy of the Sierra Leone Rise (Sites 366 and 667), *Initial Rep. Deep Sea Drill. Proj., 108*, 279-294, 1989.

Miller, K. G., J. D. Wright , and R. G. Fairbanks, Unlocking the icehouse: Oligocene-Miocene oxygen isotope, eustasy, and margin erosion, *J. Geophys. Res., 96*, 6829-6848, 1991a.

Miller , K. G., M. D. Feigenson, J. D.Wright, and B. M. Clement, Miocene isotope reference section, Deep Sea Drilling Project Site 608: An evaluation of isotope and biostratigraphic resolution, *Paleoceanography, 6*, 33-52, 1991b.

Mountain, G. S., and B. E. Tucholke, Mesozoic and Cenozoic Geology of the U.S. Atlantic Continental Slope and Rise, in *Geologic Evolution of the United States Atlantic Margin*, edited by C. W. Poag, pp. 293-341, Van Nostrand Reinhold Company, New York, 1985.

Oberhänsli, H., Latest Cretaceous - early Neogene oxygen and carbon isotopic record at DSDP sites in the Indian Ocean, *Mar. Micropaleontol., 10*, 91-115, 1986.

Oppo, D. W., and R. G. Fairbanks, Variability in the deep and intermediate water circulation of the Atlantic Ocean during the past 25,000 years: Northern Hemisphere modulation of the Southern Ocean, *Earth Planet. Sci. Lett., 86*, 1-15, 1987.

Oppo, D. W., R. G. Fairbanks, and A. L. Gordon, Late Pleistocene Southern Ocean $\delta^{13}C$ variability, *Paleoceanography, 5*, 43-54, 1990.

Ostlund, H. S., H. Craig, W. S. Broecker, and D. Spencer, *GEOSECS Atlantic, Pacific, and Indian Expedition*, vol. 7, *Shorebased Data and Graphics*, National Science Foundation, Washington, D. C., 1987.

Parsons, B., and J. G. Sclater, An analysis of the variation of ocean floor bathymetry and heat flow with age, *J. Geophys. Res., 82*, 803-827, 1977.

Pisias, N. G., N. J. Shackleton, and M.A . Hall, Stable isotope and calcium carbonate records from hydraulic piston cored Hole 574A: high-resolution records from the middle Miocene, *Initial Rep. Deep Sea Drill. Proj., 85*, 735-748, 1985.

Prentice, M. L., and R. K. Matthews, Cenozoic ice-volume history: Development of a composite oxygen isotope record, *Geology, 17*, 963-966, 1988.

Raymo, M. E., W. F. Ruddiman, J. Backman, B. M. Clement, and D. G. Martinson, Late Pliocene variation in northern hemisphere ice sheets and North Atlantic Deep Water circulation, *Paleoceanography, 4*, 413-446, 1989.

Reid, J. L., On the contribution of the Mediterranean Sea outflow to the Norwegian-Greenland Sea, *Deep Sea Res., Part A, 26*, 1199-1223, 1979.

Richardson, M. and M. A. Arthur, The Gulf of Suez - northern Red Sea Neogene rift: a quantitative basin analysis, *Mar. Petrol. Geol., 5*, 247-270, 1988.

Roberts, D. G., Marine geology of the Rockall Plateau and Trough, *Phil. Trans. Royal Soc. London, Seri. A, 278*, 447-509, 1975.

Ruddiman, W. F., Sediment redistribution on the Reykjanes

Ridge: Seismic evidence, *Geol. Soc. Am. Bull., 83*, 2039-2062, 1972.

Savin, S.M., R.G. Douglas, and F.G. Stehli, Tertiary marine paleotemperatures, *Geol. Soc. Am. Bull., 86*, 1499-1510, 1975.

Savin, S. M., G. Keller, R. G. Douglas, J. S. Killingley, L. Shaughnessy, M. A. Sommer, E. Vincent, and P. Woodruff, Miocene benthic foraminiferal isotope records: A synthesis, *Mar. Micropaleontol., 6*, 423-450, 1981.

Savin, S. M., et al., The evolution of Miocene surface and near-surface marine temperatures: Oxygen isotopic evidence, in The Miocene Ocean: Paleoceanography and Biogeography, edited by J. P. Kennett, *Mem. Geol. Soc. Am., 163*, 49-82, 1985.

Schlich, R., et al., *Proc. Ocean Drill. Prog., Initial Repts.*, vol. 120, 648pp., Ocean Drilling Program, College Station, Tex., 1989.

Schnitker, D., North Atlantic oceanography as possible cause of Antarctic glaciation and eutrophication, *Nature, 284*, 615-616, 1980.

Sclater, J. G., D. Abbott, and J. Thiede, Paleobathymetry and sediments of the Indian Ocean, in *Indian Ocean Geology and Biostratigraphy*, edited by J.R. Heirtzler, et al., pp. 25-59, AGU, Washington, D. C., 1977a.

Sclater, J. G., S. Hellinger, and C. Tapscott, The paleobathymetry of the Atlantic Ocean from the Jurassic to the present, *J. Geol., 85*, 509-552, 1977b.

Sclater, J. G., L. Meinke, A. Bennett, and C. Murphy, The depth of the ocean through the Neogene, in The Miocene Ocean: Paleoceanography and Biogeography, edited by J. P. Kennett, *Mem. Geol. Soc. Am., 163*, 1-19, 1985.

Shackleton, N. J., The carbon isotope record of the Cenozoic: History of organic carbon burial and of oxygen in the ocean and atmosphere, in *Marine Petroleum Source Rocks*, edited by H. Brooks and A. J. Fleet, pp. 423-434, Oxford Blackwell Scientific, London, 1987.

Shackleton, N. J., and J. P. Kennett, Paleotemperature history of the Cenozoic and initiation of Antarctic glaciation: Oxygen and carbon isotopic analyses in DSDP Sites 277, 279, and 281, *Initial Rep. Deep Sea Drill. Proj., 29*, 743-755, 1975.

Shackleton, N. J. and N. D. Opdyke, Oxygen isotope and paleomagnetic stratigraphy of Equatorial Pacific core V28-238: Oxygen isotope temperatures and ice volumes on a 10^5 year and 10^6 year scale, *Quat. Res., 3*, 39-55, 1973.

Shackleton, N. J., M. A. Hall, J. Line, and C. Chuxi, Carbon isotope data in core V19-30 confirm reduced carbon dioxide in the ice age atmosphere, *Nature, 306*, 319-322, 1983.

Shackleton, N. J., M. A. Hall, and A. Boersma, Oxygen and carbon isotope data from Leg 74 foraminifers, *Initial Rep. Deep Sea Drill. Proj., 74*, 599-612, 1984.

Shore, A. N., and R. Z. Poore, Bottom currents and ice rafting in the North Atlantic: Interpretation of Neogene depositional environment of Leg 49 cores, *Initial Rep. Deep Sea Drill. Proj., 49*, 859-872, 1979.

Talwani, M. and O. Eldholm, Evolution of the Norwegian-Greenland Sea, *Geol. Soc. Am. Bull., 88*, 969-999, 1977.

Tucholke, B. E. and G. S. Mountain, Tertiary paleoceanography of the western North Atlantic ocean, in *The Western North Atlantic Region, Decade of North American Geology*, vol. M, edited by P. R. Vogt and B. E. Tucholke, pp. 631-650, Geological Society of America, Boulder, Colo., 1986.

Vincent, E., and W. H. Berger, Carbon dioxide and polar cooling in the Miocene: The Monterey Hypothesis, in *The Carbon Cycle and Atmospheric CO_2: Natural Variations Archean to Present. Geophys. Monogr. Ser.*, vol. 32, edited by E. T. Sunquist and W. S. Broecker, pp. 455-468, AGU, Washington, D. C., 1985.

Vincent, E., J. S. Killingley, and W. H. Berger, The Magnetic Epoch - 6 carbon shift: A change in the ocean's $^{13}C/^{12}C$ ratio 6.2 million years ago, *Mar. Micropaleontol., 5*, 185-203, 1980.

Vogt, P. R., The Faeroe-Iceland-Greenland Aseismic Ridge and the Western Boundary Undercurrent, *Nature, 239*, 79-81, 1972.

Vogt, P. R., and O. E. Avery, Detailed magnetic surveys in the northeast Atlantic and Labrador Sea, *J. Geophys. Res. 79*, 363-389, 1974.

Weissel, J. K., D. E. Hayes, and E. M. Herron, Plate tectonics synthesis: The displacements between Australia, New Zealand, and Antarctica since the Late Cretaceous, *Mar. Geol., 25*, 231-277, 1977.

Woodruff, F., and S. R. Chambers, Mid-Miocene benthic foraminiferal oxygen and carbon isotopes and stratigraphy, Southern Ocean ODP Site 744, *Proc. Ocean Drill. Program., Sci. Results, 115*, 935-940, 1991.

Woodruff, F., and S. M. Savin, Miocene deepwater oceanography, *Paleoceanography, 4*, 87-140, 1989.

Woodruff, F., and S. M. Savin, Mid-Miocene isotope stratigraphy in the deep sea: High resolution correlations, paleoclimatic cycles, and sediment preservation, *Paleoceanography, 6*, 755-806, 1991.

Woodruff, F., S. M. Savin, and R. G. Douglas, Miocene stable isotope record: A detailed deep Pacific Ocean study and its paleoclimatic implications, *Science, 212*, 665-668, 1981.

Woodruff, F., S. M. Savin, and L. Abel, Miocene Indian Ocean benthic foraminiferal oxygen and carbon isotopes: ODP Site 709, *Proc. Ocean Drill. Program, Sci. Results, 115*, 519-528, 1990.

Worthington, L. V., The Norwegian Sea as a mediterranean basin, *Deep-Sea Res., 17*, 77-84, 1970.

Wright, J. D., and K. G. Miller, Miocene stable isotope stable isotope stratigraphy, Site 747, Kerguelen Plateau, *Proc. ODP, Sci. Results, 120*, in press, 1992a.

Wright, J. D., and K. G. Miller, Southern Ocean influences on late Eocene to Miocene deepwater circulation, *Ant. Res. Ser.*, edited by J.P. Kennett and D. Warnke, AGU, Washington D.C., in press, 1992b.

Wright, J. D, Miller, K. G., Fairbanks, R. G., Evolution of deep-water circulation: Evidence from the late Miocene Southern Ocean. *Paleoceanography, 6*, 275-290, 1991.

R. G. Fairbanks and J. D. Wright, Lamont-Doherty Geological Observatory, Columbia University, Palisades, NY 10964.

K. G. Miller, Department of Geological Sciences, Rutgers University, New Brunswick, NJ 08903.

(Received July 1, 1991;
revised March 23, 1992;
accepted April 2, 1992.)